1 **Title**

2 **Reanalysis of metabolomics data reveals that microbiota transplant therapy modulates**

3 **important fecal and plasma metabolite profiles in children with autism spectrum disorders**

4

Khemlal Nirmalkar[1,# *], Fatir Qureshi[2, 3,!,#], Dae-Wook Kang[4,], Christina K. Flynn[1,5], Juergen Hahn[2,3,6], James B. Adams[1,5], Rosa Krajmalnik-Brown[1,7 *]

[1]Biodesign Center for Health Through Microbiomes, Arizona State University, Tempe, AZ, USA

[2]Department of Biomedical Engineering, Rensselaer Polytechnic Institute, Troy, NY 12180, USA

[3]Center for Biotechnology and Interdisciplinary Studies, Rensselaer Polytechnic Institute, Troy, NY 12180, USA

[4]Department of Civil and Environmental Engineering, The University of Toledo, Toledo, OH 43606, USA

[5]School for Engineering of Matter, Transport, and Energy, Arizona State University, Tempe, AZ 85287, USA

[6]Department of Chemical and Biological Engineering, Rensselaer Polytechnic Institute, Troy, NY 12180, USA

[7]School of Sustainable Engineering and the Built Environment, Arizona State University, Tempe, AZ 85281, USA

# These authors contributed equally

! Current address: Whitehead Institute for Biomedical Research, Cambridge, MA, 02142

[*]Correspondence: Rosa Krajmalnik-Brown Dr.Rosy@asu.edu and Khemlal Nirmalkar khem@asu.edu

Keywords: Autism Spectrum Disorder (ASD), metabolites, metabolomics, Fecal Microbiota transplant (FMT), Microbiota transplant therapy (MTT)

Running Title: Reanalysis of metabolomics data for microbiota transplant therapy in Autism

Abstract:

While Autism Spectrum Disorder (ASD) is diagnosed through behavioral symptoms and psychometric evaluations, it has also been associated with distinct metabolomic patterns. A previous clinical trial of Microbiome Transplant Therapy (MTT) in children with ASD and gastrointestinal (GI) issues revealed significant differences in plasma metabolomics between children with ASD and their typically developing (TD) counterparts, which diminished after MTT. The objective of this study was to reanalyze the plasma and fecal samples using updated metabolomics libraries at Metabolon, and applying a comprehensive panel of statistical methods. This approach aimed to provide deeper insights into ASD-related metabolic differences and the impact of MTT. The reanalysis identified more statistically significant metabolites and highlighted specific metabolites whose relative peak intensities differed between the ASD and TD groups, as well as metabolites with significant changes in peak intensity post-MTT. Several plasma metabolites, including sarcosine, iminodiacetate, caproate, and caprylate, initially showed significant differences between the ASD and TD groups but shifted to resemble TD levels after MTT treatment. In fecal samples, *p*-cresol sulfate and sphingolipids emerged as metabolites with altered intensities following MTT treatment. Multivariate Fisher's Discriminant Analysis (FDA) with leave-one-out cross-validation revealed that a set of metabolites—including p-cresol sulfate, hydroxyproline, and caprylate—could robustly classify the ASD and TD cohorts pre-treatment. However, after treatment, the same FDA model could not distinguish the two groups, as the FDA scores became similar to those of the TD cohort.

Our findings enhance the understanding of ASD-associated metabolic changes and highlight the potential of MTT to influence these profiles. This underscores the importance of reanalysis using updated databases and robust statistical methods for comparative analysis. Further studies with larger cohorts and placebo-controlled trials are necessary to validate these results and explore the biochemical pathways involved, paving the way for personalized treatment approaches.

Introduction

In the past decade, the prevalence of autism spectrum disorder (ASD) in the United States has significantly increased, with 1 in 31 children now diagnosed (CDC, 2025). Individuals with ASD experience social communication and behavioral impairments (Adams et al., 2011; Lord et al., 2018), and often have persistent gastrointestinal (GI) issues, such as constipation and diarrhea (Adams et al., 2011; Hung et al., 2023). These co-occurring conditions correlate with increased ASD behavioral severity (Adams et al., 2011), prompting research intersecting their relationship with the gut-brain axis and gut microbiome.. Studies reveal significant differences in gut microbiome compositions between ASD individuals and typically developing (TD) children, including higher levels of *Clostridia* species and lower levels of beneficial microbes like *Bifidobacterium* (Kang et al., 2019; Morton et al., 2023).

The complex interaction among microbes, influenced by their metabolites, has been hypothesized to affect GI and behavioral symptoms in ASD (Adams et al., 2011; Krajmalnik-Brown et al., 2014; Kang et al., 2020; Needham et al., 2021; Morton et al., 2023; Hung et al., 2023; Zheng et al., 2023). Differences in metabolite profiles in fecal, urine, and blood samples have been reported in ASD individuals compared to TD peers (Gabriele et al., 2014; Kang et al., 2018; 2020; Needham et al., 2021; Zheng et al., 2021). For example, elevated levels of fecal short-chain fatty acids and blood glutamate, along with increased blood gamma-aminobutyric acid (GABA), have been observed in people with ASD (Shinohe et al., 2006; Kang et al., 2018; El-Ansary et al., 2014; Khalifa et al., 2019). GABA and glutamate, which are critical for cognition and mood regulation, show an altered levels in ASD individuals, suggesting an underlying neuroinflammation (El-Ansary et al., 2014). Additionally, other gut-derived metabolites, such as p-cresol and p-cresol sulfate, are found at higher levels in ASD individuals' urine, feces, or serum (Flynn et al., 2025; Kang et al., 2018; De Angelis et al., 2013; Gabriele et al., 2014).

Given the microbiome-gut-ASD interconnection, Microbiota Transplant Therapy (MTT) has been explored for its potential benefits in ASD (Kang et al., 2017). Microbiota Transplant Therapy, (redefined from microbiota transfer therapy, Takyi et al. 2025) has shown promise in addressing GI issues and reducing behavioral severity in ASD children. An open-label study by

Kang et al. reported an 80% reduction in GI symptoms and a 24% decrease in core ASD symptoms post-MTT, with sustained improvements over two years (Kang et al., 2017, 2019). Increases in beneficial microbes such as *Bifidobacterium*, *Prevotella*, and *Desulfovibrio* were also noted (Kang et al., 2017, 2019).

Building on these findings, untargeted metabolomics of fecal and plasma samples from the same individuals in the MTT study identified several plasma metabolites significantly lower in the ASD group at baseline, including nicotinamide riboside, IMP, iminodiacetate, methylsuccinate, galactonate, valylglycine, sarcosine, and leucylglycine, while caprylate and heptanoate were higher (Kang et al., 2020). Though no fecal metabolite showed significant baseline differences, *p*-cresol sulfate levels were non-significantly higher in ASD children and decreased after MTT (Kang et al., 2020). Multivariate analysis highlighted significant metabolite changes post-MTT, with improvements in sarcosine and inosine 5'-monophosphate in plasma (Adams et al., 2019) and a model of indole, imidazole, propionate, adenosine, and hydroxyproline achieving 96% accuracy in distinguishing ASD from TD children (Qureshi et al., 2020).

In this study, we reanalyzed the metabolomics data collected for the Kang et al. 2017 and 2019 studies. We extend upon the findings reported by Kang et al. (2020) by expanding the scope of metabolomics data analyzed through Metabolon's updated metabolomics libraries and robust statistical methods. Utilizing more up-to-date algorithms and libraries for metabolite detection, we offer a comprehensive comparison of metabolite profiles, encompassing nucleotides, neurotransmitters, amino acids, xenobiotics, and lipids derived from human plasma and fecal samples collected from a carefully matched cohort of individuals with ASD and typically developing children. Previously, data was analyzed using univariate tests and principal-component analysis (PCA) and correlation analysis for selective metabolites. In this reanalysis, we not only replicated the prior analysis techniques, but we also explored other methods such as contrasting the area under the receiver operating characteristic curve (AUROC) between groups, random forest, and Fisher discriminant analysis (FDA) to revalidate the findings (Fig. 1). The results reveal significant differences in metabolite levels between TD and ASD baseline groups in plasma and feces, which were previously unidentified, and important changes shifting the ASD metabolon towards TD after MTT.

Methods

Study design, sample collection and data processing

This study extends the work of Kang et al. (2020) by performing a more thorough reanalysis of plasma and fecal metabolomics data collected before and after MTT in children with ASD. The original protocol was approved by the U.S. Food and Drug Administration (FDA) (investigational new drug number 15886) and the Institutional Review Board of Arizona State University (ASU IRB protocols #00001053 and #00004890). The trial was registered at ClinicalTrials.gov (NCT02504554), as described in Kang et al. (2017, 2020). Study participants, consent, MTT, and sample collections were described in detail in our previous studies (Kang et al., 2017; 2020). In brief, 20 typically developing (TD) children and eighteen children with ASD were recruited, in the age range of 7-16 years old. Children with ASD participated in an open-label clinical trial including vancomycin for 2 weeks, one-day bowel cleanse with MoviPrep, followed by 7-8 weeks of MTT and Prilosec (a stomach acid suppressant), and a follow-up at 8 weeks post-treatment (i.e., 18 weeks from Day 0) (Kang et al., 2017).

For metabolomic analysis, we collected plasma samples at ASD baseline, week 3 (after the vancomycin and bowel cleanse and just before the first dose of microbiota), and week 10 (the end of MTT treatment) (Fig. 1). We had one missing plasma sample in week 3. Fecal samples were collected at baseline, week 3 (right after an initial dose of microbiota), week 10 and week 18 (8 weeks after the end of MTT). For TD children, we collected plasma and feces only at baseline as they were not treated. All samples were frozen immediately after collection, shipped in dry ice to ASU, and stored at -80°C. Demographic, medical data and diet history was recorded, as described by Kang *et al*., 2017, 2020. Aliquoted frozen samples were analyzed by Metabolon Inc. (Durham, NC, USA) using ultrahigh-performance liquid chromatography-tandem mass spectroscopy (UHPLC-MS/MS) instruments for untargeted metabolomics.

This reanalysis leverages upgrades in peak identification algorithms, software, and libraries available to Metabolon Inc. (https://www.metabolon.com/). In feces, a total of 1,068 metabolites were detected across all samples. Of these, 825 metabolites (77.3%) were chemically identified and assigned a metabolite name, while the remaining 243 features (22.7%) were unnamed. Similarly, in the plasma samples, a total of 1,001 metabolites were detected, with 844 (84.3%) chemically identified and 157 (15.7%) remaining unnamed.

Their proprietary software integrates the mass spectrometry data with retention time alignment, isotope pattern analysis, and database matching to enhance metabolite annotation accuracy. In total, 5,400 compounds were detectable via untargeted metabolomics, with available annotations. Raw data underwent imputation and z-score normalization according to the methods described by Kang et al., 2020. Using these extended approaches new data were generated, resulting in modified abundances of metabolites (peak area/intensity) and the identification of additional metabolites within the samples. To focus the analysis on identified compounds for biological interpretation, metabolites lacking chemical annotations (e.g., unidentified compounds labeled as 'X-###') were excluded from downstream analysis.

It is important to note that, we recorded xenobiotics ~16% in plasma and ~18% in feces which was 1% higher than our previous study (Kang et al., 2020). The slight increase likely reflects updates in Metabolon's annotation libraries during reanalysis. Importantly, Metabolon's xenobiotic category encompasses a broad range of compounds, including not only exogenous chemicals (e.g., drugs, pollutants) but also microbial co-metabolites, dietary constituents, and plant-derived compounds. For instance, gut-derived metabolites such as p-cresol and 4-ethylphenyl sulfate are classified by metabolon as xenobiotics due to their chemical features and involvement in pathways like benzoate metabolism. Therefore, the relatively high proportion of xenobiotics observed here may reflect the microbiome-influenced metabolic landscape of individuals with autism, rather than an overrepresentation of exogenous exposures.

Univariate analysis

Initially, univariate hypothesis testing was employed to compare metabolites between groups. Depending on the data distribution and type of relationship of the two groups, the most appropriate statistical test was selected. Mann-Whitney was utilized for comparing non-parametric data with similar distributions between the TD and ASD samples, while a t-test was used in alternative cases. When comparing ASD groups at various time points a Wilcoxon sign-rank test was used for non-parametric distributions and a paired t-test was used for parametric distributions. False discovery rates (FDR) were determined using the leave-one-out (LOO) approach. This technique is well-suited for high-dimensional data that has an underlying correlational structure, as is common in metabolic studies (Arici et al., 2025). This method applies the same hypothesis testing approach to every combination of a dataset with one sample

excluded. Then, the proportion of significant findings is determined to evaluate the likelihood of false discovery. Subsequently, findings with $p < 0.05$ and FDR <0.05 were considered statistically significant.

Area Under the Receiver Operating Characteristic Curve (*AUROC)*

The area under the receiver operating characteristic curve (AUROC) was used to assess the degree to which metabolite measurements were discernible between pre-treatment and post-treatment time points. For a binary classification task, the AUROC is determined by plotting the true positive rate (TPR) against the false positive rate (FPR) of a model across varying threshold values. The area under the TPR/FNR plot corresponds to the AUROC and can serve as a metric to quantify the degree to which different groups are separable. The AUROC value ranges from 0 to 1, where a value of 0.5 indicates no discrimination, a value of 1 represents perfect discrimination, and a value close to 0 suggests that the model is performing worse than random, potentially predicting the opposite of the true outcome.

The AUROC was calculated by treating the measurements of each metabolite individually as the classifier input, which was subject to a threshold value. AUROC was determined for each fecal and plasma metabolite, with baseline measurements being compared against all other time points. The measurements collected from the ASD group were also compared against the TD measurements, both in their entirety and on a time-point basis. By assessing all the AUROC values generated for each metabolite between baseline, week3, and week10 vs TD across, the average fecal and plasma AUROC values for each group were determined.

Fisher's Discriminant Analysis (FDA)

FDA is a dimensionality reduction technique that aims to find a transformation of the original data that accentuates the differences between distinct groups while reducing the variations within each group. This method projects multidimensional data into a lower dimensional space in such a way as that dissimilar groups are maximally separated, while members of the same group remain closely grouped together. By doing so, FDA facilitates the creation of more discriminative representations (Huberty, 1975).

Metabolites that had been deemed to be statistically significant in both plasma and feces were used to develop an FDA model for the purpose of classification between ASD and TD

cohorts. To mitigate the risk of overfitting, feature selection was limited to five variables, as literature suggests this approach optimally suits small sample sizes with similar data structure properties in ASD prediction. This decision is also supported by the success of prior fecal and plasma model panels achieving the upper bounds of their predictive accuracy with this number of features (Howsmon et al., 2017; Vargason et al., 2019; Qureshi et al., 2020). An exhaustive search of all potential FDA model combinations of five metabolites was determined, using only the ASD baseline and TD groups as training data. For all possible combinations of five metabolites, the AUROC was evaluated to determine whether to conduct further testing. Each metabolite combination model that achieved an AUROC greater than 0.97 was subjected to a leave-one-out cross-validation (LOO-CV) paradigm. The top-performing model, as quantified by CV accuracy, was then used to predict the classification of the MTT week3 and week10 groups.

Random Forest Analysis

Random forest (RF) is defined as an ensemble learning method that can be used for classification. An RF approach to classification operates by aggregating the collective performance of multiple decision trees and using the plurality of outcomes to predict the group label of a sample. This algorithm is constructed by first setting aside one-third of the training data to utilize as testing data for cross-validation purposes. Subsequently, a user-specified number of decision trees is constructed. The performance of the algorithm is then quantified based on the classification accuracy on the randomly selected test set. A random forest model was fit using all significant metabolomic measurements in order to evaluate the mean decrease in accuracy for the exclusion of each variable. This metric is commonly utilized to provide a perspective on feature importance, which can be used to more efficiently identify variables better suited for distinguishing between labeled categories (Altman et al., 2017). Although random forests are generally more effective with larger datasets, they can still serve as exploratory tools for feature selection in smaller datasets, provided their limitations are acknowledged and results are interpreted cautiously (Wouter et al., 2013)

Correlation Coefficient

The Pearson‘s correlation coefficient is defined by the strength and direction of the linear relationship between two continuous variables. The Pearson’s correlation coefficient was

240 determined between all metabolite, pathway, and taxa pairs. The significance of the correlation
241 coefficients was evaluated using hypothesis testing with a significance level set at $\alpha = 0.05$. The
242 robustness of significant findings was cross validated using a LOO approach. Employing this
243 strategy, the significance of the correlation coefficient was determined for all possible
244 combinations of the input measurement with a single sample removed. If a false discovery rate
245 (FDR) of less than 0.05 was determined, the finding was deemed to be significant.
246
247 All univariate analysis, area under the receiver operating characteristic (AUROC), random forest
248 analysis and plots were made with Python (v3.8.5) in Jupyter Notebook (v6.1.4) using numpy
249 (v1.19.2), matplotlib (v3.3.2), seaborn (v0.11.0), pandas (v1.1.3) and scipy (v1.5.2). PCA plot
250 was made using MetaboAnalyst v6.0 (https://www.metaboanalyst.ca/). BioRender (Biorender,
251 2022, Licensed, https://biorender.com) and Inkscape (v1.1) were used to create or edit the
252 figures.
253
254 **Results**
255 In the previous study (Kang et al., 2020), 621 plasma and 666 fecal metabolites were identified
256 in the collected samples. However, through reprocessing and reanalysis of the metabolomics data
257 using new updated reference library, a greater number of biochemical compounds were
258 identified from the same samples. We identified a total of 844 plasma and 825 fecal metabolites,
259 and most of the newly identified metabolites in plasma and feces were lipids, amino acids, or
260 xenobiotics (Fig. 2).
261
262 ***Metabolite profiles changed after MTT in ASD children***
263 Univariate analyses showed that certain metabolites that were initially different between ASD
264 and TD groups at baseline, and shifted following MTT. These metabolites relative peak intensity
265 changed post-treatment, and some of these intensities became similar to those in TD in plasma
266 (Fig. 3A, C) and fecal samples (Fig. 3B, Supplementary S1). In plasma, out of 844 metabolites,
267 we observed 20 metabolites whose intensity was significantly different between the ASD
268 baseline and TD and that also changed after MTT (Fig. 3A). We grouped these plasma
269 metabolites into two clusters; **1)** Cluster P-high (cluster of 14 plasma metabolites), which
270 includes metabolites that had significantly higher intensity (adjusted $p<0.05$) at ASD baseline vs

271 TD, but after MTT, the relative intensity of these metabolites decreased and became similar to
272 TD (Fig. 3A). Figure 3A shows 12 plasma metabolites in this category, including:
273 glycerophosphoethanolamine (GPEA), caprylate (8:0), and caproate (6:0). The other two plasma
274 metabolites, taurine and adenosine-5'-monophosphate (AMP), were non-significantly higher
275 (p>0.05) at baseline vs TD but significantly decreased after MTT (Fig. 3A). **2)** Cluster P-low
276 (cluster of 6 plasma metabolites) which includes metabolites that had significantly lower
277 intensity (adjusted p<0.05) at baseline vs TD, but after MTT, relative intensity of these
278 metabolites significantly increased (adjusted p<0.05) and became similar to TD. Cluster P-low
279 includes sarcosine, iminodiacetate, bilirubin, 2-methylserine, and indole propionate.
280 Similar to plasma, out of 825 fecal metabolites, we observed 22 metabolites that had
281 significantly different intensities from TD or changed after MTT (Fig 3B, Supplementary Fig.
282 S1). Fecal metabolites were also divided into two clusters; **1)** Cluster F-low (cluster of 3 fecal
283 metabolites) where all metabolites had significantly lower intensity (adjusted p<0.05) at baseline
284 vs. TD, and **2)** Cluster F-high (cluster of 19 fecal metabolites) where all metabolites had higher
285 intensity (adjusted p<0.05) at baseline vs. TD. Cluster F-low (Fig. 3B-) shows 3 fecal
286 metabolites pentadecanoate (15:0), myristate (14:0), and carboxyethyl-GABA whose intensity
287 was significantly lower at baseline vs. TD, and only one metabolite pentadecanoate (15:0) whose
288 intensity significantly increased (adjusted p<0.05) after week18 (Fig. 3B). In cluster F-high, 19
289 metabolites had significantly higher intensity (adjusted p<0.05) at baseline vs TD, here the
290 intensity of 5 metabolites: p-cresol sulfate, theobromine, oxalate ethanedioate, dodecanedioate
291 (C12), and Urolithin-A significantly decreased (adjusted p<0.05) at week3 vs baseline (Fig. 3B).
292 The intensity of N-palmitoyl-sphingosine (d18:1/16:0), p-cresol sulfate, eicosanoyl-sphingosine
293 (d20:1), hydroxyproline, theobromine, N-stearoyl-sphingosine (d18:1/18:0), N-oleoyl-
294 sphingosine (d18:1/18:1), 3-methyl-2-oxobutyrate, dodecanedioate (C12), and D-urobilin
295 significantly decreased after week18 compared to baseline. We did not observe any significant
296 change for week10 vs. baseline (Fig. 3B).
297
298 ***Analytics and Patterns of Differential Metabolomic Composition Appear Similar between***
299 ***Feces and Plasma***
300 We utilized AUROC, PCA analysis and random forest analysis to categorize the differences in
301 metabolomic composition across groups and timepoints. AUROC was calculated for all 20

302 plasma and 22 fecal metabolites that were significantly different between ASD baseline and TD.
303 To examine how metabolites differed post-MTT, AUROC was recalculated at all time points
304 between the ASD and TD cohorts. The average AUROC for all 20 plasma metabolites was 0.73
305 comparing ASD baseline vs TD, and ASD baseline vs after week3, and week10 AUROC's were
306 0.70 and 0.62 respectively (Fig. 4A). When we compared the MTT group with TD, after week3
307 and week10, we observed that the plasma profile became more similar to TD with AUROC 0.56
308 for week3 vs TD and 0.59 for week10 vs TD (Fig. 4A). A similar trend was also observed for 22
309 fecal metabolites, which were initially observed with an average AUROC of 0.74 for ASD
310 baseline vs TD. After MTT, fecal metabolite profiles became more similar to the TD group, with
311 AUROC values of 0.58 for week3 vs TD and 0.61 for week10 vs TD (Fig. 4B). Overall, the
312 observed shift in AUROC values for plasma and fecal metabolites indicates that after MTT, the
313 metabolic composition in plasma and fecal samples from children with ASD became more
314 similar to their TD counterparts.
315 PCA analysis showed that relative intensity of the 20 significant plasma metabolites at
316 baseline were distinct from TD, but after MTT, became much more similar to TD (Fig. 4C).
317 Fecal samples exhibited greater variance in the typically developing group compared to their
318 ASD counterparts in the first two principal components, and this pattern was also observed in the
319 post treatment ASD group (Supplementary Fig. S2). Random forest was used as a
320 complimentary method to validate the assessment of each metabolites relative utility in
321 distinguishing between cohorts. Using the full list of metabolites, it was possible to achieve
322 accuracies greater than 0.95. The mean decrease in accuracy for the ASD status prediction model
323 indicated that both fecal and plasma metabolites had a similar influence on model performance
324 (Supplementary Fig. S3). The top 10 features contributing to mean decrease in accuracy were
325 split evenly between the plasma and fecal metabolites, potentially offering complementary
326 insights into discerning ASD and TD samples. (Supplementary Fig. S4).
327
328 ***MTT changed metabolites abundance in ASD towards TD***
329 We selected four plasma metabolites that were highly significantly different at baseline and
330 showed changes after MTT (Fig. 5).. A lysine derivative sarcosine and iminodiacetate (IDA)
331 were significantly lower (adjusted $p<0.05$) at baseline vs. TD. However, after week3 (after
332 vancomycin) and week10 (MTT) the relative intensity was observed to significantly increase

333 (adjusted $p<0.05$) and became more similar to TD (Fig. 3A, 5A-B). To quantify the changes, we
334 calculated the AUROC, and sarcosine's intensity showed 0.82 AUROC at baseline vs TD, at
335 week3 (AUROC=0.73) and at week10 (AUROC=0.85) compared. baseline (Fig. 6A). Notably,
336 the AUROC at week3 and week10 compared to TD were 0.56 and 0.52, respectively (Fig. 6A),
337 which indicates that after MTT, sarcosine's relative intensity became similar to TD. Similar
338 findings were observed for iminodiacetate (Fig. 6B).
339 In contrast, we observed two medium chain fatty acids in plasma, caproate (6:0) and caprylate
340 (8:0), that were significantly higher at baseline vs TD, but after week3 and week10 (MTT)
341 significantly decreased (adjusted $p<0.05$) and their abundances became similar to TD (Fig. 5C-
342 D). Caproate and caprylate AUROCs were 0.78 for baseline vs TD, which showed further
343 differences comparing baseline to week3 (AUROC caproate=0.83, caprylate=0.79) and week10
344 (AUROC caproate=0.88, caprylate=0.90) vs. baseline, but the AUROC at week3 and week10 vs.
345 TD was between 0.51-0.65 (Fig. 6C-D), which also indicates that after MTT, the relative
346 intensity of caproate and caprylate became similar to TD.
347 In feces, phenolic compound *p*-cresol sulfate, theobromine, and three sphingolipids; N-
348 palmitoyl-sphingosine (d18:1/16:0), N-stearoyl-sphingosine (d18:1/18:0), and N-oleoyl-
349 sphingosine (d18:1/18:1) were significantly higher at baseline vs TD but after week3 (right after
350 an initial dose of microbiota), week10 (MTT) and week18 (after 8 weeks of MTT) significantly
351 decreased vs. baseline and became similar to TD (Fig 3B, Fig. 7A-D). AUROC calculation
352 showed that baseline vs. TD had 0.76 for *p*-cresol sulfate, after baseline vs. week3
353 AUROC=0.80, vs week10 AUROC=0.66, vs week18 AUROC=0.75, which indicates after MTT,
354 *p*-cresol sulfate profile changed in children with ASD (Fig. 8A). Interestingly, *p*-cresol sulfate
355 AUROC for TD vs. week3; TD vs. week10; TD vs. week18 were in the range 0.55-0.60 (Fig.
356 8A), indicating that after MTT, *p*-cresol sulfate peak relative intensity became similar to TD.
357 Similarly, theobromine, N-palmitoyl-sphingosine (d18:1/16:0), N-stearoyl-sphingosine
358 (d18:1/18:0), and N-oleoyl-sphingosine (d18:1/18:1) had higher AUROC after MTT vs. ASD
359 baseline and lower AUROC values after MTT vs. TD, indicating important changes from
360 baseline and greater similarity to TD measurements (Fig. 8B-D). Overall, AUROC validate the
361 findings from univariate analysis and showed the differences between the groups for plasma and
362 fecal metabolites.
363

364 ***FDA models revealed five key metabolites that notably changed after MTT and became similar***
365 ***to TD***
366 Univariate hypothesis testing identified 20 plasma metabolites and 22 fecal metabolites whose
367 intensities significantly differed between TD and ASD cohorts at baseline or changed after
368 microbiota transplant therapy (MTT) (Fig. 3). Both sets of metabolites were used to separately
369 construct multivariate statistical models *via* FDA using all possible combinations of 3, 4, and 5
370 variables to distinguish between ASD and TD cohorts. The top-performing FDA model made up
371 exclusively of plasma metabolites included, 2-palmitoyl-GPC (16:0), caprylate (8:0), laurate
372 (12:0), bilirubin, and indolepropionate achieving an AUROC of 0.99 and a leave-one-out cross-
373 validated (LOO-CV) accuracy of 95%. Similarly, the plasma metabolite data was used to
374 develop an FDA model, with significant features selected through the same univariate approach.
375 The optimal plasma model incorporated *p*-cresol sulfate, hydroxyproline, theobromine, N-oleoyl-
376 sphingosine (d18:1/18:1), and 1-methylhistidine.
377 Utilizing the complete set of 44 significantly differing metabolites from both plasma and
378 feces, all possible 5-metabolite FDA models were also constructed. Through LOO-CV, a model
379 consisting of *p*-cresol sulfate (feces), hydroxyproline (feces), caprylate (plasma),
380 indolepropionate (plasma), and bilirubin (plasma) was identified as the most robust, with a cross-
381 validation accuracy of 95% (Fig. 4D). This model exhibited a type I error rate of 3% and a type
382 II error rate of 0%. Notably, the performance of all multivariate models for classifying between
383 ASD and TD status significantly declined after MTT, as did the measurements taken at the two-
384 year follow-up. The metabolite peak intensities in the model showed significant convergence
385 towards the TD group, with the difference between the median of the five metabolites relative
386 intensity values decreasing by 88% between week 0 and week18, compared to the TD group.
387
388 ***Fecal p-cresol and p-cresol sulfate are positively correlated***
389 We conducted correlation analyses to examine the relationship between certain fecal and plasma
390 metabolites. Fecal *p*-cresol and fecal *p*-cresol sulfate were significantly positively correlated
391 ($p<0.001$, Pearson-R=0.75) (Supplementary Fig. S5). Fecal *p*-cresol and fecal *p*-cresol sulfate
392 did not show a significant correlation with plasma *p*-cresol sulfate (Supplementary Fig. S6-7),
393 which suggests that gut permeability or other factors may affect how much *p*-cresol leaves the
394 gut. *p*-cresol was not detected in plasma, which is not surprising since it has very low solubility

395 in aqueous solutions. We performed correlation analyses with previously published taxonomic
396 and metabolic pathways (KEGG orthologs) (Nirmalkar et al., 2022), but did not observe
397 statistically significant correlations.
398
399 **Discussion**
400 A distinct metabolic signature has been consistently observed in plasma and fecal samples
401 collected from children with ASD (Kang et al., 2020; Needham et al., 2021). While several
402 underlying biochemical pathways and environmental factors contribute to these differences,
403 MTT not only improved GI and behavioral symptoms associated with ASD (Kang et al., 2017,
404 2019) but also leads to a convergence of ASD metabolite profiles towards those observed in TD
405 samples (Kang et al., 2020). Reanalysis of absorbance peaks by Metabolon Inc. using a more
406 comprehensive database (see raw data in supplementary file 2), and improvement in our data
407 analysis pipeline allowed for an increase in the number of metabolites detected in plasma and
408 feces (Supplementary Fig. S2) compared to our previous measurements (Kang et al., 2020).
409 Through reanalysis, we identified 844 metabolites in plasma, and 825 metabolites in feces (Fig.
410 2), which is a substantial increase in identified metabolites from the original study. Furthermore,
411 several biochemical compounds showed notable shifts in plasma and fecal metabolic profiles
412 after MTT in ASD children. Following treatment, 20 metabolites in plasma and 22 in feces
413 whose peak intensities were initially dissimilar to TD became similar to TD (Fig. 3).
414 For plasma metabolites, we found similar results to Kang et al., 2020 for bilirubin (an
415 oxidant), iminodiacetate (xenobiotic and a glycine derivative) (Lin et al. 2019), and sarcosine (a
416 glycine derivative, and beneficial against depression and schizophrenia) (Tsai et al., 2004). The
417 relative intensities of these compounds were significantly lower at baseline but increased
418 significantly after MTT in children with ASD (Fig. 2). Also, the intensity of caprylate (8:0, a
419 medium-chain fatty acid) was higher at baseline and significantly decreased after MTT. The
420 analysis for these metabolites shows the consistency of the data previously reported by Kang et
421 al. (2019) and improvement of plasma metabolite profiles after MTT in children with ASD.
422 However, with this re-analysis we detected some potentially important metabolites, such as
423 caproate (6:0, a medium-chain fatty acid), phospholipids such as glycerophosphocholine (GPC),
424 phosphoethanolamine (PEA), glycerophosphoethanolamine (GPEA), and 2-palmitoyl-GPC
425 (16:0). The relative intensity of these metabolites was higher at baseline and significantly

426 decreased after MTT in children with ASD (Fig. 3A). Kang et al. postulated that a decrease in
427 medium-chain fatty acids, such as caprylate to be correlated with an improvement in ASD
428 symptoms (Kang et al., 2020).

429 Phospholipids are lipids that are highly abundant in neuronal membranes (Joensuu et al.,
430 2020), and they are an important source of energy and provide long-chain polyunsaturated fatty
431 acids (LC-PUFAs). Some research suggests that dysregulated phospholipid metabolism may be a
432 biological component of neurodevelopmental disorders like ASD (Pastural et al., 2009; Tamji et
433 al., 2010; El-Ansary et al. 2011; Brown et al., 2011; Ventura et al., 2020; Needham et al., 2021).
434 Increased sphingolipid-1-PO_4, a type of phospholipid that was observed in ASD serum compared
435 to TD (Wang et al., 2016). In our fecal samples, relative intensities of sphingosines N-palmitoyl-
436 sphingosine (d18:1/16:0), N-stearoyl-sphingosine (d18:1/18:0), and N-oleoyl-sphingosine
437 (d18:1/18:0) (also called ceramides) were significantly higher at ASD baseline compared to TD
438 but after MTT, they significantly decreased, and their abundance became similar to TD (Fig.
439 3B). These lipids are important for phospholipid metabolism and mitochondrial function (Tamji
440 & Crawford, 2011). However, the differential abundance of these mitochondrial markers in fecal
441 and plasma metabolites in children with ASD suggests potential mitochondrial dysfunction in
442 children with ASD and may contribute to ASD severity (Needham et al., 2021; Pastural et al,
443 2009; Rossignol & Frye, 2012; Griffiths & Levy, 2017; Lombard, 1998).

444 In plasma, GPC (phospholipid) levels were significantly higher in children with ASD
445 compared to their TD counterparts. While GPC levels decreased following MTT, the change was
446 not statistically significant (Fig 3A). Similarly, Needham et al reported that GPC was
447 significantly higher in ASD children's plasma samples and was associated with mitochondrial
448 dysfunction (Needham et al., 2021). GPC is a phospholipid-containing choline found in human
449 milk (Dangat & Johsi, 2023) and is an important nutrient for memory, mood, and muscle
450 regulation. However, administration of GPC has been shown to improve cognition against
451 dementia and Alzheimer's disease (AD) (Amenta et al., 2014; Sagaro et al., 2023). In animal
452 studies, administration of GPC was found to release acetylcholine in rat brains, elevate dopamine
453 and serotonin levels in the frontal cortex, and enhance cognitive function (Traini et al., 2020).
454 Despite the beneficial roles of phospholipids containing choline, increased GPC levels in our
455 samples from children with ASD suggest dysregulation in phospholipid metabolism, and it has

been reported that elevated levels of GPC+phosphocholines (PC) can be associated with bipolar disorder patients (Cao et al., 2017).

Another plasma metabolite, indolepropionate (IPA or Indole-3-propionate), was significantly lower at baseline compared to TD (Fig. 3A). IPA is a gut microbiota-derived metabolite of tryptophan, and is increasingly recognized for its neuroprotective and anti-inflammatory properties. In this study, IPA was significantly lower in children with ASD at baseline compared to TD controls, suggesting a potential deficiency in beneficial microbial activity or a disrupted microbial-host interface. Previous studies have reported similarly lower IPA levels in ASD animal models and in children with intrauterine growth restriction (Wang et al., 2023). Interestingly, IPA levels did not significantly change following MTT, indicating that this metabolite may be less responsive to short-term microbial interventions. The persistent reduction (non-significantly) in IPA highlights the need for further investigation into specific microbial contributors and whether longer-term or targeted interventions could restore its production and potential neuroprotective effects in ASD.

In feces, *p*-cresol and *p*-cresol sulfate have consistently emerged as metabolites of interest due to their elevated presence in the urine and feces of children diagnosed with ASD (Altieri et al., 2011, Chen et al., 2013; Kang et al., 2018; Daneberga et al., 2022; Diémé et al., 2015; Emond et al., 2013; Gevi et al 2016; Gevi et al., 2020, Li et al., 2018; Mussap et al., 2020; Osredkar et al., 2023; Perisco & Napolioni 2013, Piras et al., 2022; Tevzadze et al., 2017; Timperio et al., 2022; Flynn et al., 2025). The primary source of *p*-cresol in the body is its production by gut bacteria and act as an antimicrobial compound (Saito et al., 2019). *p*-cresol is produced *via* tyrosine metabolism and is considered a uremic toxin (Candleliere et al., 2022). To eliminate *p*-cresol from the body, the host liver carries out sulfation andforms*p*-cresol sulfate which increases its solubility so that it can be more easily excreted from the body (Gryp et al., 2017; Spanogiannopoulos et al., 2016; Clayton et al., 2009).

We observed that peak intensity of fecal *p*-cresol sulfate was significantly higher at ASD baseline compared to TD (Fig. 3B, 7A). After MTT, *p*-cresol sulfate decreased significantly, and its intensity became more similar to TD (Fig. 3B, Fig. 7A). However, we did not observe significant differences or changes between groups for *p*-cresol in feces, *p*-cresol sulfate for plasma, and *p*-cresol was not detected in plasma. Recent mouse studies have shown that when *p*-

487 cresol was administered, mice exhibited social behavior deficits and more repetitive behavior
488 relative to controls (Bermudez-Martin et al., 2021), and subsequent fecal microbiota transplant
489 from healthy mice led to normalization of ASD-like symptoms (Bermudez-Martin et al., 2021).
490 These findings suggest that *p*-cresol and/or *p*-cresol sulfate may contribute to the
491 pathophysiology of autism. Current results led to a hypothesis that MTT helps to reduce the *p*-
492 cresol sulfate levels by remodeling the gut microbial ecology in ASD children and allowing the
493 growth of microbiota from healthy donors. Another sulfated metabolite that has been associated
494 with ASD in other studies, is 4-ethylphenyl sulfate (4EPS) (Hsiao et al., 2013; Needham et al.,
495 2021; Stewart Campbell et al., 2022). While we did not detect 4EPS in fecal samples, wealso did
496 not observe significant differences or changes between groups in plasma samples. Recent clinical
497 trials in children with ASD using AB-2004, an adsorbent, showed decreased *p*-cresol sulfate and
498 4EPS levels in urine. These changes occurred alongside improvements in ASD-like behaviors,
499 suggesting 4EPS and *p*-cresol sulfate could be correlated with behavioral severity in ASD
500 (Stewart Campbell et al., 2022).

501 In feces, another interesting microbial metabolite, Urolithin-A was significantly higher at
502 baseline compared to TD (Fig. 3B). Although Urolithin A is a gut microbiota-derived metabolite
503 produced from dietary ellagitannins found in fruits such as pomegranates and berries (García-
504 Villalba et al., 2013; Selma et al., 2014), its elevated levels at baseline in individuals with ASD
505 may reflect a dysbiotic microbiota enriched in urolithin-producing taxa despite the self-restricted
506 diets commonly observed in ASD. After MTT, the introduction of a more balanced microbial
507 community likely reduced these specialized microbes, leading to lower Urolithin-A levels but no
508 statistical change except at week3 (Fig. 3B). We hypothesize that the high Urolithin-A levels in
509 ASD may be a marker of dysbiosis rather than of beneficial microbial function, and further
510 studies are required to confirm the microbial drivers of Urolithin-A production and its biological
511 relevance in ASD.

512 It is important to note that certain metabolites such as theobromine and cetirizine (Fig.
513 3B), while statistically significant between groups, reflect exogenous intake (e.g., chocolate,
514 allergy medications) rather than underlying biological shifts. Their appearance underscores the
515 importance of controlling or at least documenting for diet, medication use, and seasonal

516 variation, which should be explored in future studies with larger, placebo-controlled cohorts and
517 dietary monitoring.

518 Our most robust multivariate FDA model was composed of five metabolites from either
519 plasma or fecal samples; *p*-cresol sulfate (feces), hydroxyproline (feces), caprylate (plasma),
520 indole-propionate (plasma), and bilirubin (plasma), that were significantly different at baseline
521 vs TD and became similar to TD after MTT (Fig. 3A-B). Fecal *p*-cresol sulfate emerged as a
522 recurring component in many of the top-performing multivariate FDA models. Univariate
523 analysis demonstrated strong differences in the composition of *p*-cresol sulfate between the ASD
524 baseline and TD groups, achieving an AUROC of 0.76. These differences were utilized in the
525 linear multivariate models relying on this variable, highlighting *p*-cresol sulfate as a potentially
526 relevant biomarker for ASD in feces. Higher caprylate (plasma), and lowerindole-propionate
527 (plasma), and lower bilirubin (plasma) were also observed in the previous study (Kang et al.,
528 2020) at baseline and after MTT, relative intensity became similar to TD levels. Indole-
529 propionate, a gut metabolite has been found to be associated with ASD in humans (Yu et al.,
530 2020) and animal models (Wang et al., 2023; Jiang et al., 2024). Hydroxyproline, another FDA
531 model-identified metabolite (Fig. 4D), was previously identified at significantly higher relative
532 intensity in the plasma of children with ASD (Chen et al., 2024).

533 Combining plasma and fecal metabolite datasets resulted in higher cross-validated accuracy than
534 using either dataset alone, potentially as a consequence of complimenting biological insight
535 provided by each source. The FDA models developed for the reanalysis demonstrated an
536 accuracy of 95%, outperforming previous work with fecal metabolites from the same study,
537 which achieved an accuracy of 94.7% (Qureshi et al., 2020). Previous assessments of plasma
538 metabolites have also shown comparable capabilities to distinguish between ASD and TD
539 cohorts using linear classifier techniques (Howsmon et al., 2017; Adams et al., 2019). This prior
540 work also highlighted that after MTT treatment, the predictive accuracy and average AUROC of
541 fecal metabolites decreased substantially (Qureshi et al., 2020). This pattern was observed in the
542 metabolomic panels composed of both plasma and fecal samples in this study as well, suggesting
543 that improvements in several metabolites may have compromised their predictive validity.
544 Although cross-validation demonstrates the robustness of these findings, the influence of
545 geographic covariates on microbiome composition should be assessed to determine the broader

546 applicability of these results (Falony et al., 2016). Future studies should incorporate external
547 validation with different cohorts with a large dataset and longitudinal sampling to confirm the
548 reproducibility and clinical applicability of these models. No consistent metabolite alterations
549 were observed across plasma and fecal samples. This may reflect differential host–microbiota
550 interactions, underscoring the complexity of cross-compartmental signaling. Furthermore,
551 studies involving larger cohorts with a placebo arm, along with mechanistic investigations, will
552 be important to better elucidate the metabolic dynamics in ASD and ensure the broader clinical
553 relevance of MTT's impact.

554 Although the initial shifts in the metabolic profile observed by week 3 reflect the effects
555 of vancomycin treatment, our data suggest that these changes alone do not fully explain the
556 sustained alignment with the TD group seen after MTT. Notably, plasma metabolites remained
557 similar to TD profiles at week 18, indicating that MTT may help stabilize or maintain these
558 shifts. Also, we observed only modest changes in fecal metabolites by week 3 (after a high-dose
559 of microbiota), with clearer transitions toward TD-like profiles occurring after 8 weeks of MTT.
560 These findings are consistent with Sandler et al. (Sandler et al., 2000), where vancomycin led to
561 temporary improvements in autism symptoms, but these improvements were lost post-treatment,
562 potentially due to lack of recolonization by beneficial microbes. In contrast, our results show that
563 MTT may preserve or reinforce beneficial shifts initiated by antibiotics. This interpretation is
564 consistent with prior findings in recurrent *Clostridioides difficile* infection (Zhou et al., 2023)
565 and highlights the need to consider both antibiotic and transplant contributions in interpreting
566 longitudinal metabolomic responses. In conclusion, the reanalysis of plasma and fecal
567 metabolites revealed an additional 223 plasma and 159 fecal metabolites compared to the
568 previous report by Kang et al., 2020. The contrast in metabolite composition before and after
569 MTT groups provides insight on metabolites with potential biological relevance in children with
570 autism and/or GI issues. This research underscores the value of re-analysis when databases
571 improve and the importance of investigating non-behavioral features in ASD diagnosis and
572 provides valuable insights into the intricate metabolic landscape of this complex disorder.

573 Using different analysis methods, we consistently observed that sarcosine,
574 iminodiacetate, caproate, and caprylate in plasma were significantly different in ASD vs TD, as
575 reported previously. However, we also identified phospholipids such as
576 glycerophosphoethanolamine (GPE), glycerophosphocholine (GPC), and phosphoethanolamine

in plasma, as well as fecal sphingosines N-palmitoyl-sphingosine (d18:1/16:0), N-stearoyl-sphingosine (d18:1/18:0), and N-oleoyl-sphingosine (d18:1/18:0), which were significantly different at baseline compared to typically developing (TD) individuals and/or changed after MTT. Moreover, we observed that fecal *p*-cresol sulfate was higher at baseline compared to TD and decreased significantly after MTT.

Notably, *p*-cresol sulfate in feces was consistently found across our different statistical methods as a potential biomarker before and after MTT in children with ASD. This suggests the potential of microbially-produced metabolite in affecting ASD symptoms. Larger cohort and placebo-controlled trials are necessary to validate our findings and unravel the mechanisms underlying MTT in ameliorating aberrant metabolomic profiles associated with ASD. Furthermore, insights into the underlying biochemical pathways will facilitate the development of more tailored treatment strategies.

Additional Information: The Supplementary Material for this article can be found online at:

Data Availability.

The clinical data used in this study are available from the previously published work by Kang et al. (Kang et al. 2019, 2020). The metabolomics datasets analyzed in this manuscript are provided in the supplemental material file 2-3.

Code Availability.

No custom code was developed for this study, except for FDA analysis (Fig.4D) which can be found at https://github.com/FatirQureshi/FDA-Model-Search. All analyses were performed using standard software packages, as described in the Methods section of the manuscript.

Abbreviations:

1. **4EPS** - 4-Ethylphenyl Sulfate
2. **AMP** - Adenosine-5'-Monophosphate
3. **ASD** - Autism Spectrum Disorder
4. **AUROC** - Area Under the Receiver Operating Characteristic Curve

5. **CV** - Cross validation
6. **FDA** - Fisher's Discriminant Analysis (context-dependent, could also mean Food and Drug Administration)
7. **FDR** - False Discovery Rate
8. **GABA** - Gamma-Aminobutyric Acid
9. **GC-MS** - Gas Chromatography-Mass Spectrometry
10. **GI** - Gastrointestinal
11. **GPC** - Glycerophosphocholine
12. **GPEA** - Glycerophosphoethanolamine
13. **IMP** - Inosine 5'-Monophosphate
14. **KEGG** - Kyoto Encyclopedia of Genes and Genomes
15. **LC-PUFA** - Long-Chain Polyunsaturated Fatty Acid
16. **LOO** - Leave-One-Out
17. **LOO-CV** - Leave-One-Out Cross-Validation
18. **MTT** - Microbiota Transplant Therapy
19. **PC** - Phosphocholine
20. **PCA** - Principal Component Analysis
21. **PEA** - Phosphoethanolamine
22. **TD** - Typically Developing
23. **UHPLC-MS/MS** - Ultrahigh-Performance Liquid Chromatography-Tandem Mass Spectroscopy

Authors Contributions

Conceptualization, K.N., D.W.K., J.B.A., R.K.B.; Data curation, K.N, F.Q., J.B.A., R.K.B.; Formal analysis, K.N, F.Q., J.B.A., R.K.B.; Funding acquisition, D.W.K., J.B.A., R.K.B.; Investigation, K.N, F.Q., J.B.A., R.K.B.; Methodology, K.N., J.H., J.B.A., R.K.B.; Project administration, R.K.B., J.B.A.; Software, K.N.; F.Q.; Supervision, D.W.K., J.H., J.B.A., R.K.B.; Visualization, K.N., F.Q.; Writing—original draft, K.N., F.Q., J.B.A., R.K.B.; Writing—review & editing, , K.N., F.Q., D.W.K., J.H., J.B.A., R.K.B.

Disclosure/Conflict of interest

K.N., J.B.A. D. -W.K. and R.K.-B. have pending/approved patents for autism biomarkers and the use of FMT for various conditions, including autism. J.B.A. and R.K.-B are co-founders of Autism Diagnostics LLC and Gut-Brain Axis Therapeutics. The other authors declare no competing interests.

Acknowledgments

We thank all children with ASD and typically developing children for participating in the study as well as the children's families for their support on the study. We thank Biodesign Center for Health Through Microbiomes Start-up at Arizona State University for the financial support and Joel Meraz for assisting with the references. This work was supported by Finch Therapeutics (formerly Crestovo) to obtain the metabolomics data set.

654

655 **Figures:**

656

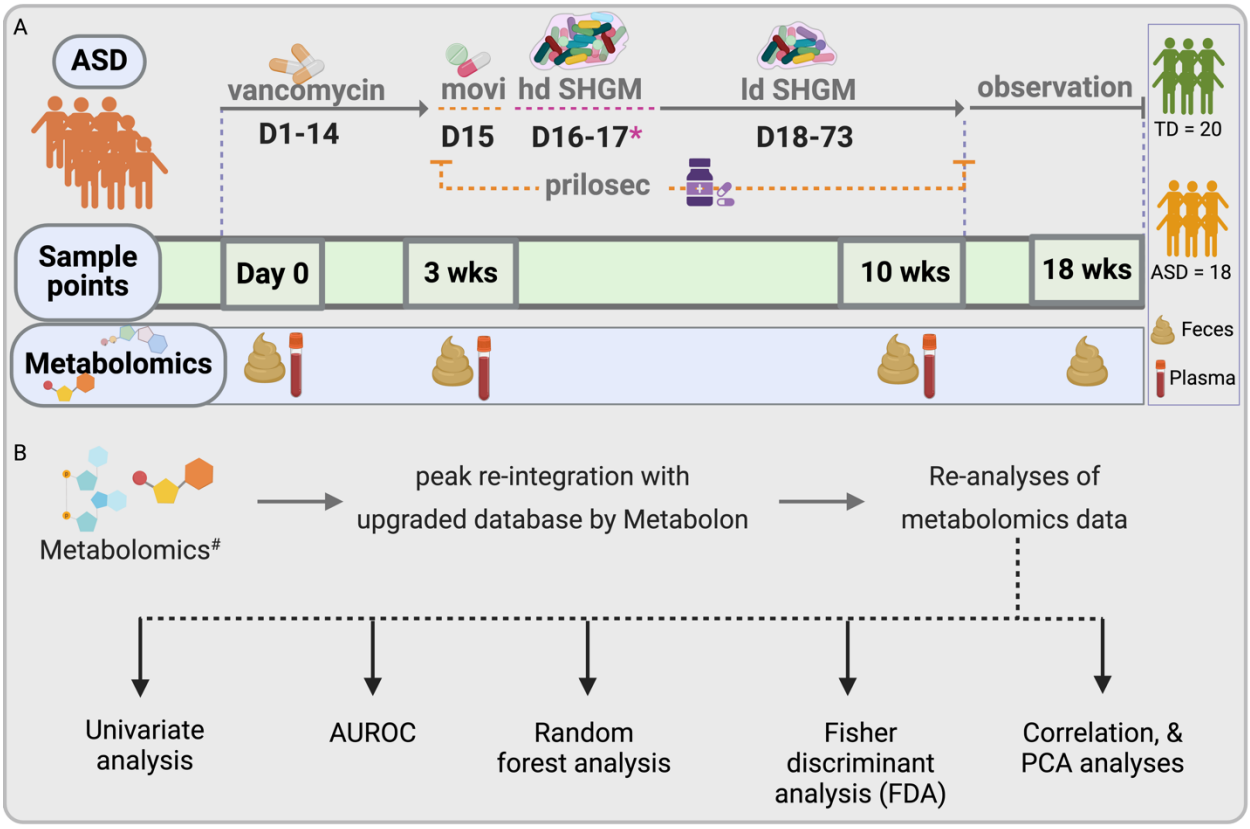

657

658

659 **Figure 1**: The study design of microbiota transplant therapy for fecal and plasma metabolomics (A) and

660 the overview of the data analyses for fecal and plasma metabolites (B).

661 Plasma was collected right before high-dose microbiota and feces were collected right after high-dose

662 microbiota.

663

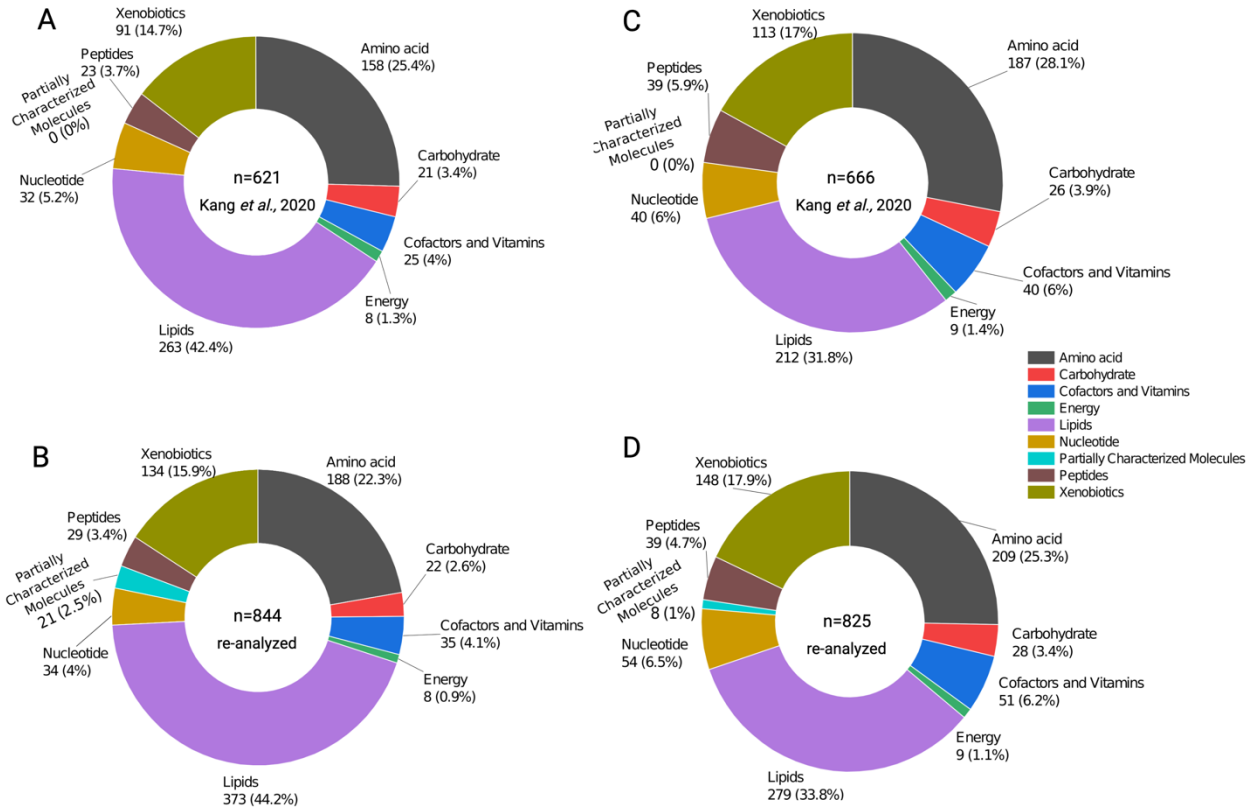

Figure 2. An overview of plasma metabolomics with the previous A) and re-analyzed B), fecal metabolomics with the previous C) and re-analyzed D) of peaks. The pie charts show the total number of metabolites identified and the type of metabolites in plasma and fecal samples.

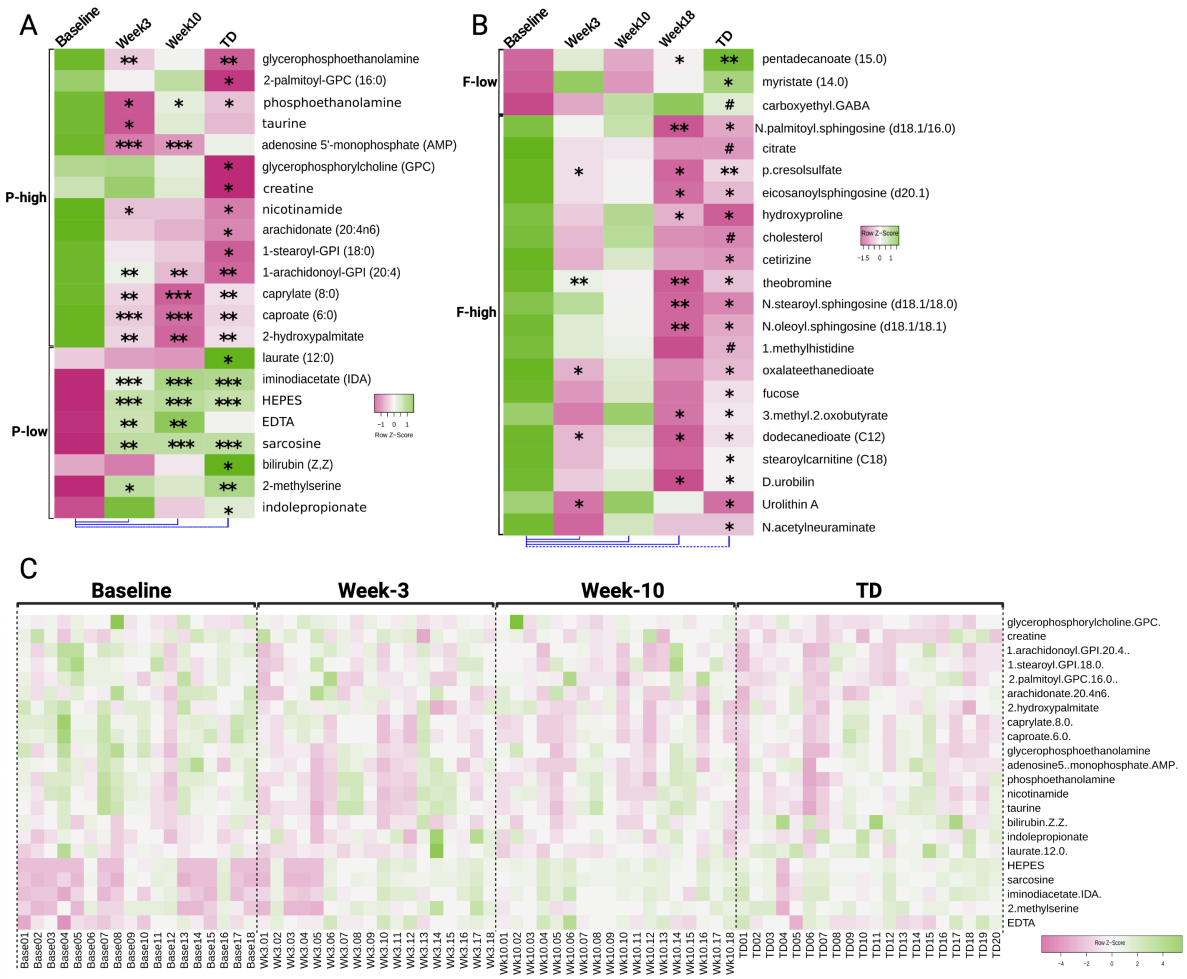

Figure 3. Univariate comparison of the (z-score) relative intensity of plasma (A) and fecal (B) metabolites in children with ASD and comparisons after MTT and with TD. For the plasma metabolites (A), a longitudinal paired-wise univariate analysis was performed at baseline vs. week3, week10 and cross-sectional unpaired comparison vs. TD. Similarly, for the fecal metabolites (B), a longitudinal paired-wise univariate analysis was performed (shown in solid blue lines at the bottom of the heatmap) at baseline vs. week3, week10, week18 and cross-sectional unpaired comparison vs. TD (shown in dashed blue line). (C) heatmap (z-score) for each participant with 20 plasma metabolites that were significantly changed or were different in children with ASD at baseline compared with MTT and with TD groups in Figure 3A. Week18 time was not available for the plasma. See Supplementary Fig. S1 for fecal metabolites heatmap for each participant. The median of relative intensities in plasma (A) and feces (B) was used to construct the heatmap for each group. *Single asterisk indicates $p < 0.05$, **double asterisks indicate $p < 0.01$, triple *** asterisks indicate $p < 0.001$. # indicates the statistically significant ($p<0.05$)

684 metabolites after log-transformation. All p-values are FDR corrected. ASD: Autism Spectrum Disorders,
685 TD: Typically Developing.

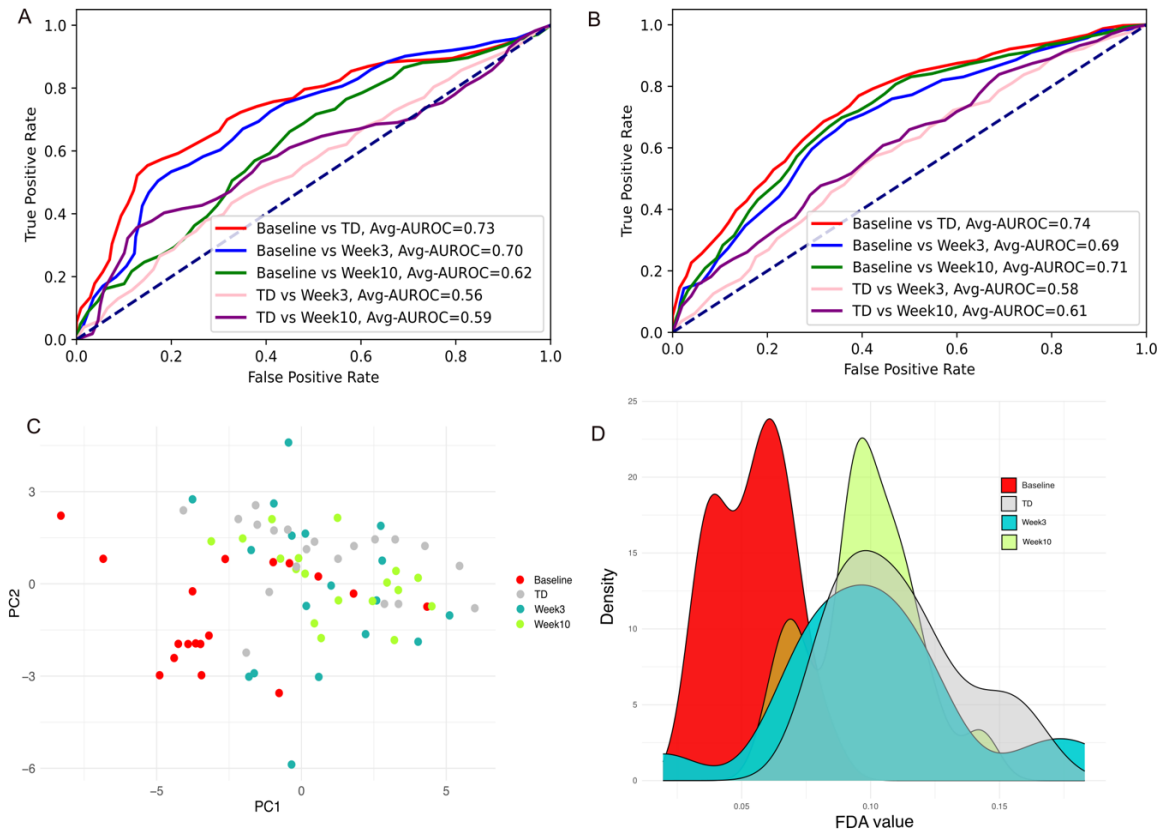

Figure 4. An average Receiver operating characteristic curves (AUROC) of A) plasma, B) fecal metabolites, C) principal component analysis (PCA) of plasma metabolites, and D) FDA analysis of fecal and plasma metabolites (*p*-cresol sulfate, caprylate (C:8) bilirubin, indolepropionate and hydroxyproline) using probability density curves associated with FDA scores before and after MTT in ASD, and TD children. For FDA analysis, true positive vs false positive rate was determined across all threshold values to characterize between ASD Baseline against all possible alternative groups. For AUROC and PCA plots, 22 fecal and 20 plasma metabolites (presented in Figure 3) were used. Refer to Supplementary Figure S2 for PCA plot for fecal metabolites. ASD – autism spectrum disorder, MTT - microbiota transplant therapy, TD - typically developing, FDA - Fisher discriminant analysis.

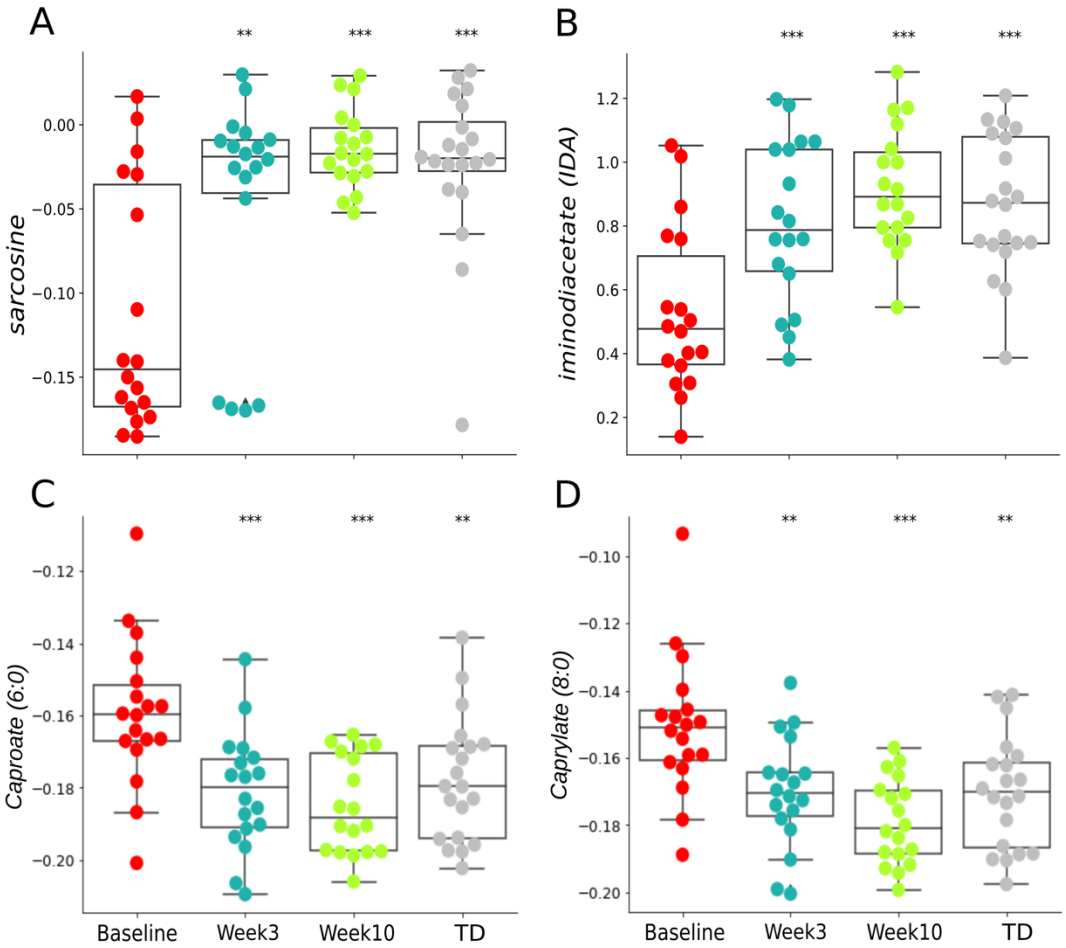

Figure 5. Univariate comparison of the relative intensity (after log10 transformation) in plasma for A) Sarcosine, B) Iminodiacetate (IDA), C) Caproate (6:0), and D) Caprylate (8:0) at ASD baseline vs. MTT (week3, week10) and TD. Each colored dot represents one ASD individual, and grey colored dots represent TD. Asterisks represent significant differences between ASD baseline, and the other groups (*Single asterisk indicates p <0.05, **double asterisks indicate p<0.01, ns not significant, all p-values are FDR corrected). ASD: Autism Spectrum Disorders, TD: Typically Developing.

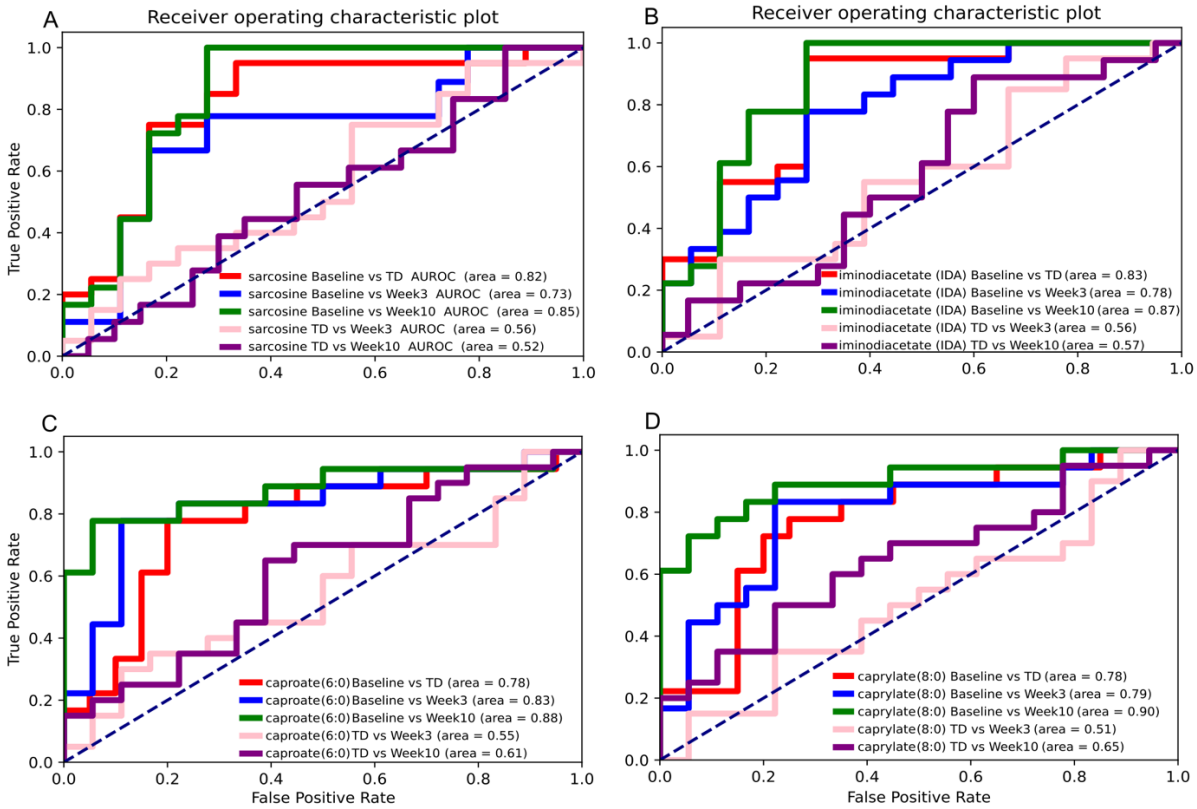

Figure 6. Receiver operating characteristic curves (AUROC) of A) Sarcosine, B) Iminodiacetate (IDA), C) Caproate (6:0), and D) Caprylate (8:0) for ASD baseline vs. MTT (week3, week10) and TD. True positive vs false positive rate was determined across all threshold values to characterize between ASD Baseline against all possible alternative groups.

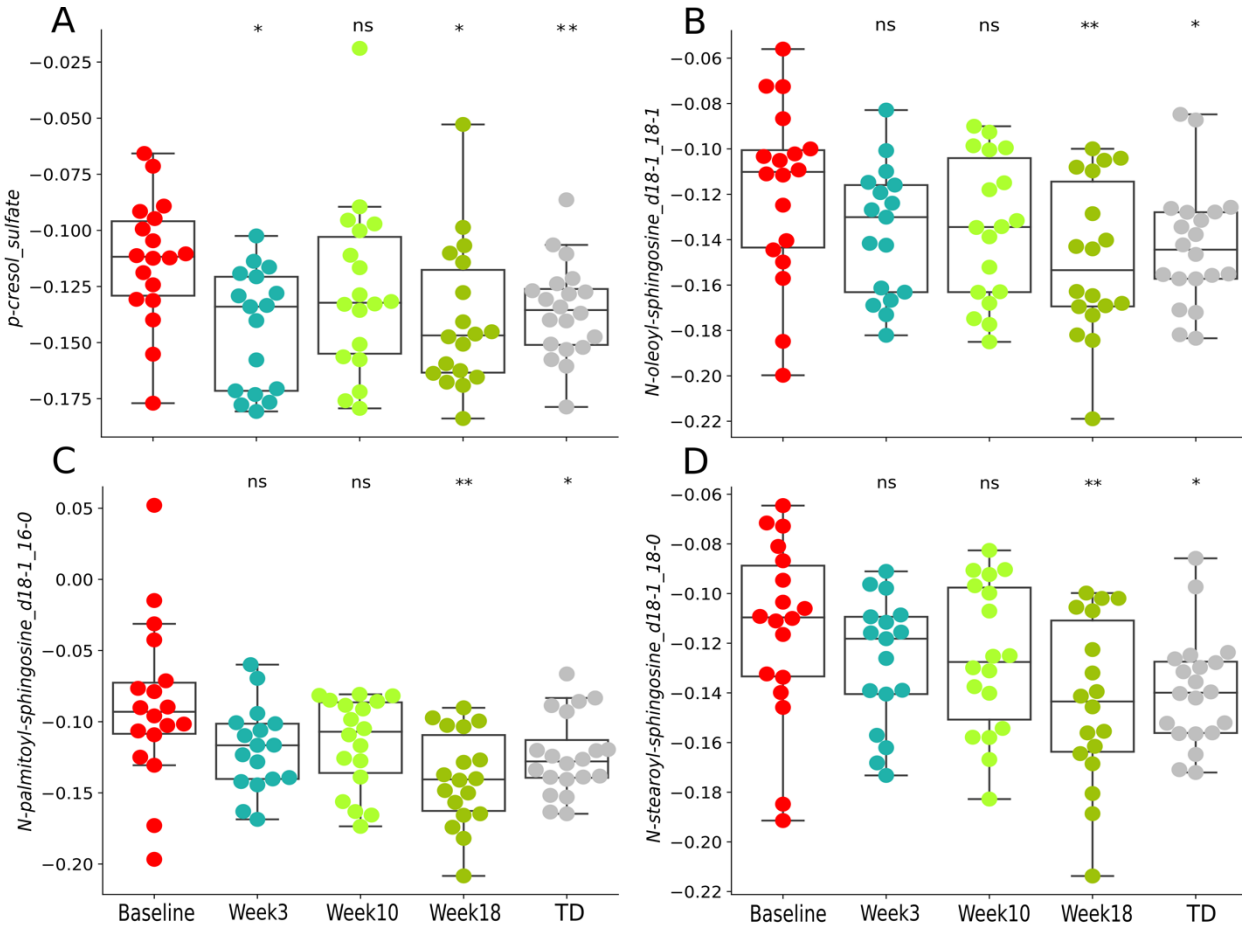

Figure 7. Univariate comparison of the relative intensity (after log10 transformation) in feces for A) p-cresol sulfate, B) N-oleoyl-sphingosine (d18:1/18:1), C) N-palmitoyl-sphingosine (d18:1/16:0), and D) N-stearoyl-sphingosine (d18:1/18:0) at ASD baseline vs. MTT (week3, week10, week18) and TD. Each colored dot represents one ASD individual and grey colored dots represent TD. Asterisks represent significant differences between ASD baseline and the other groups (*Single asterisk indicates $p < 0.05$, **double asterisks indicate $p<0.01$, ns not significant, all p-values are FDR corrected). ASD: Autism Spectrum Disorders, TD: Typically Developing.

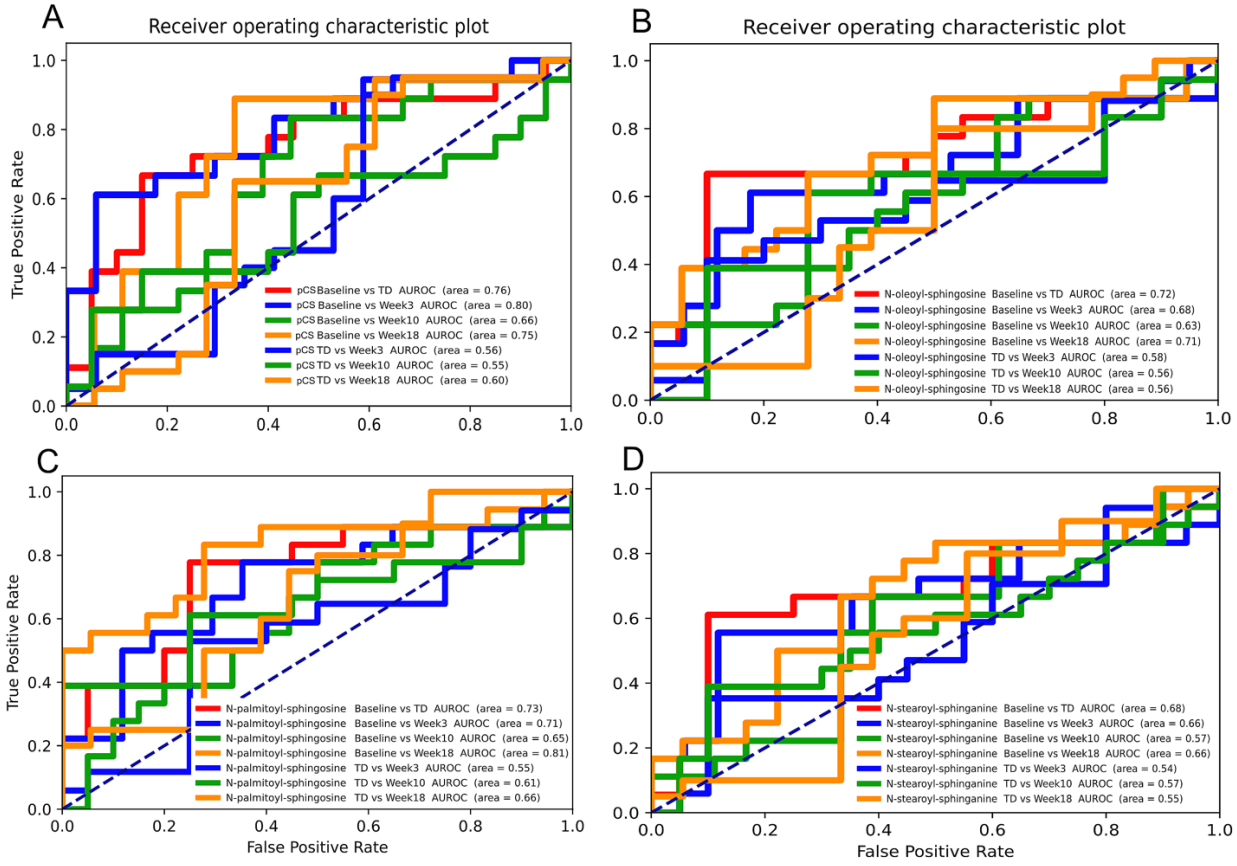

Figure 8. Receiver operating characteristic curves (AUROC) of A) p-cresol sulfate, B) (N-oleoyl-sphingosine d18:1/18:1), C) N-palmitoyl-sphingosine (d18:1/16:0), and D) N-stearoyl-sphingosine (d18:1/18:0) at ASD baseline vs. MTT (week3, week10, week18) and TD. True positive vs false positive rate was determined across all threshold values to characterize between ASD baseline against all possible alternative groups. pCS - p-cresol sulfate.

References:

1. Adams JB, Johansen LJ, Powell LD, Quig D, Rubin RA. Gastrointestinal flora and gastrointestinal status in children with autism – comparisons to typical children and correlation with autism severity. BMC Gastroenterol. 2011a. doi:10.1186/1471-230X-11-22.
2. Adams JB, Audhya T, McDonough-Means S, Rubin RA, Quig D, Geis E, Gehn E, Loresto M, Mitchell J, Atwood S, Barnhouse S, Lee W. Nutritional and metabolic status of children with autism vs. neurotypical children, and the association with autism severity. Nutr Metab (Lond). 2011b ;8(1):34. doi: 10.1186/1743-7075-8-34. PMID: 21651783; PMCID: PMC3135510.
3. Adams, J.B.; Vargason, T.; Kang, D.-W.; Krajmalnik-Brown, R.; Hahn, J. Multivariate Analysis of Plasma Metabolites in Children with Autism Spectrum Disorder and Gastrointestinal Symptoms Before and After Microbiota Transfer Therapy. *Processes* **2019**, *7*, 806. https://doi.org/10.3390/pr7110806.
4. Altieri, L., Neri, C., Sacco, R., Curatolo, P., Benvenuto, A., Muratori, F., Santocchi, E., Bravaccio, C., Lenti, C., Saccani, M., Rigardetto, R., Gandione, M., Urbani, A., & Persico, A. M. (2011). Urinary p-cresol is elevated in small children with severe autism spectrum disorder. Biomarkers, 16(3), 252–260. https://doi.org/10.3109/1354750X.2010.548010
5. Altman, N., Krzywinski, M. Ensemble methods: bagging and random forests. Nat Methods 14, 933–934 (2017). https://doi.org/10.1038/nmeth.4438
6. Amenta F, Carotenuto A, Fasanaro AM, Rea R, Traini E. The ASCOMALVA (Association between the Cholinesterase Inhibitor Donepezil and the Cholinergic Precursor Choline Alphoscerate in Alzheimer's Disease) Trial: interim results after two years of treatment. J Alzheimers Dis. 2014;42 Suppl 3:S281-8. doi: 10.3233/JAD-140150
7. Arici H, Qureshi FA, Mulmule J, Hahn J. 2025. Multiple hypothesis testing for pre-screening of factor selection for classification of high-dimensional data. *J Process Control* 152:103469. https://doi.org/10.1016/j.jprocont.2025.103469.

767 8. Bermudez-Martin, P., Becker, J.A.J., Caramello, N. et al. The microbial metabolite p-
768 Cresol induces autistic-like behaviors in mice by remodeling the gut microbiota.
769 Microbiome 9, 157 (2021). https://doi.org/10.1186/s40168-021-01103-z.
770 9. Brown CM, Austin DW. Autistic disorder and phospholipids: A review. Prostaglandins
771 Leukot Essent Fatty Acids. 2011 Jan-Feb;84(1-2):25-30. doi:
772 10.1016/j.plefa.2010.09.007. PMID: 20970971.
773 10. Cao, B., Stanley, J., Passos, I. *et al.* Elevated Choline-Containing Compound Levels in
774 Rapid Cycling Bipolar Disorder. *Neuropsychopharmacol* **42**, 2252–2258 (2017).
775 https://doi.org/10.1038/npp.2017.39
776 11. CDC. 2023-ADDM-Factsheet_508; 2023. https://www.cdc.gov/autism/data-
777 research/index.html .
778 12. Chen, Q., Qiao, Y., Xu, X. J., Tao, Y., & You, X. (2019). Urine organic acids as potential
779 biomarkers for autism-spectrum disorder in chinese children. Frontiers in Cellular
780 Neuroscience, 13. https://doi.org/10.3389/fncel.2019.00150
781 13. Chen, WX., Chen, YR., Peng, MZ. et al. Plasma Amino Acid Profile in Children with
782 Autism Spectrum Disorder in Southern China: Analysis of 110 Cases. J Autism Dev
783 Disord 54, 1567–1581 (2024). https://doi.org/10.1007/s10803-022-05829-z
784 14. Clayton TA, Baker D, Lindon JC, Everett JR, Nicholson JK. Pharmacometabonomic
785 identification of a significant host-microbiome metabolic interaction affecting human
786 drug metabolism. Proc Natl Acad Sci U S A. 2009 Aug 25;106(34):14728-33. doi:
787 10.1073/pnas.0904489106. Epub 2009 Aug 10. PMID: 19667173; PMCID:
788 PMC2731842.
789 15. Created in BioRender. Krajmalnik-brown, R. (2022) https://BioRender.com/x41x091.
790 16. Daneberga, Z., Nakazawa-Miklasevica, M., Berga-Svitina, E., Murmane, D., Isarova, D.,
791 Cupane, L., Masinska, M., Nartisa, I., Lazdane, A., & Miklasevics, E. (2022). Urinary
792 organic acids spectra in children with altered gut microbiota composition and autistic
793 spectrum disorder. Nordic Journal of Psychiatry, 76(7), 523–529.
794 https://doi.org/10.1080/08039488.2021.2014954
795 17. Dangat K, Joshi S. *Breast Milk and Cognitive Performance in Children*. Elsevier Inc.;
796 2023. https://www.sciencedirect.com/science/article/abs/pii/B9780323898348000143

797 18. De Angelis M., Piccolo M., Vannini L., Siragusa S., De Giacomo A., Serrazzanetti D.I.,
798 Cristofori F., Guerzoni M.E., Gobbetti M., Francavilla R. Fecal microbiota and
799 metabolome of children with autism and pervasive developmental disorder not otherwise
800 specified. PLoS ONE. 2013;8:e76993. doi: 10.1371/journal.pone.0076993.
801 19. Diémé, B., Mavel, S., Blasco, H., Tripi, G., Bonnet-Brilhault, F., Malvy, J., Bocca, C.,
802 Andres, C. R., Nadal-Desbarats, L., & Emond, P. (2015). Metabolomics Study of Urine in
803 Autism Spectrum Disorders Using a Multiplatform Analytical Methodology. Journal of
804 Proteome Research, 14(12), 5273–5282.
805 20. El-Ansary AK, Bacha AG, Al-Ayahdi LY. Impaired plasma phospholipids and relative
806 amounts of essential polyunsaturated fatty acids in autistic patients from Saudi Arabia.
807 Lipids Health Dis. 2011 Apr 22;10:63. doi: 10.1186/1476-511X-10-63. PMID: 21513514;
808 PMCID: PMC3107801.
809 21. El-Ansary, A., Al-Ayadhi, L. GABAergic/glutamatergic imbalance relative to excessive
810 neuroinflammation in autism spectrum disorders. J Neuroinflammation 11, 189 (2014).
811 https://doi.org/10.1186/s12974-014-0189-0
812 22. Emond P, Mavel S, Aïdoud N, Nadal-Desbarats L, Montigny F, Bonnet-Brilhault F,
813 Barthélémy C, Merten M, Sarda P, Laumonnier F, Vourc'h P, Blasco H, Andres CR. GC-
814 MS-based urine metabolic profiling of autism spectrum disorders. Anal Bioanal Chem.
815 2013 Jun;405(15):5291-300. doi: 10.1007/s00216-013-6934-x. Epub 2013 Apr 10.
816 PMID: 23571465.
817 23. Falony G, Joossens M, Vieira-Silva S, Wang J, Darzi Y, Faust K, Kurilshikov A, Bonder
818 MJ, Valles-Colomer M, Vandeputte D, Tito RY, Chaffron S, Rymenans L, Verspecht C,
819 De Sutter L, Lima-Mendez G, D'hoe K, Jonckheere K, Homola D, Garcia R, Tigchelaar
820 EF, Eeckhaudt L, Fu J, Henckaerts L, Zhernakova A, Wijmenga C, Raes J. 2016.
821 Population-level analysis of gut microbiome variation. *Science* 352(6285):560–564.
822 https://doi.org/10.1126/science.aad3503.
823 24. Flynn CK, Adams JB, Krajmalnik-Brown R, et al. Review of Elevated Para-Cresol in
824 Autism and Possible Impact on Symptoms. Int J Mol Sci. 2025;26(4):1513. Published
825 2025 Feb 11. doi:10.3390/ijms26041513.

826 25. Gabriele S, Sacco R, Cerullo S, et al. Urinary p -cresol is elevated in young French
827 children with autism spectrum disorder: a replication study. Biomarkers. 2014;19(6):463-
828 470. doi:10.3109/1354750X.2014.936911.
829 26. García-Villalba R, Beltrán D, Espín JC, Selma MV, Tomás-Barberán FA. Time course
830 production of urolithins from ellagic acid by human gut microbiota. J Agric Food Chem.
831 2013;61(37):8797-8806. doi:10.1021/jf402498b
832 27. Gevi, F., Zolla, L., Gabriele, S., & Persico, A. M. (2016). Urinary metabolomics of young
833 Italian autistic children supports abnormal tryptophan and purine metabolism. Molecular
834 Autism, 7, 47. https://doi.org/10.1186/s13229-016-0109-5.
835 28. Gevi, F., Belardo, A., & Zolla, L. (2020). A metabolomics approach to investigate urine
836 levels of neurotransmitters and related metabolites in autistic children. Biochimica et
837 Biophysica Acta (BBA) - Molecular Basis of Disease, 1866(10), 165859.
838 https://doi.org/10.1016/j.bbadis.2020.165859
839 29. Golubeva AV, Joyce SA, Moloney G, Burokas A, Sherwin E, Arboleya S, Flynn I,
840 Khochanskiy D, Moya-Pérez A, Peterson V, Rea K, Murphy K, Makarova O, Buravkov
841 S, Hyland NP, Stanton C, Clarke G, Gahan CGM, Dinan TG, Cryan JF. Microbiota-
842 related Changes in Bile Acid & Tryptophan Metabolism are Associated with
843 Gastrointestinal Dysfunction in a Mouse Model of Autism. EBioMedicine. 2017
844 Oct;24:166-178. doi: 10.1016/j.ebiom.2017.09.020. Epub 2017 Sep 21. PMID:
845 28965876; PMCID: PMC5652137.
846 30. Gorrindo P, Williams KC, Lee EB, et al. Gastrointestinal dysfunction in autism: parental
847 report, clinical evaluation, and associated factors. Autism Res 2012; 5(2):101–8.
848 31. Griffiths KK, Levy RJ, Evidence of Mitochondrial Dysfunction in Autism: Biochemical
849 Links, Genetic-Based Associations, and Non-Energy-Related Mechanisms. Oxid. Med.
850 Cell. Longev 2017 (2017), doi:10.1155/2017/4314025. - DOI - PMC - PubMed
851 32. Gryp T, Vanholder R, Vaneechoutte M, Glorieux G. p-Cresyl Sulfate. Toxins (Basel).
852 2017 Jan 29;9(2):52. doi: 10.3390/toxins9020052. PMID: 28146081; PMCID:
853 PMC5331431.
854 33. Hashimoto, K. Emerging role of the host microbiome in neuropsychiatric disorders:
855 overview and future directions. Mol Psychiatry 28, 3625–3637 (2023).
856 https://doi.org/10.1038/s41380-023-02287-6

857 34. He, J., Gong, X., Hu, B. et al. Altered Gut Microbiota and Short-chain Fatty Acids in
858 Chinese Children with Constipated Autism Spectrum Disorder. Sci Rep 13, 19103 (2023).
859 https://doi.org/10.1038/s41598-023-46566-2
860 35. Howsmon DP, Kruger U, Melnyk S, James SJ, Hahn J. Classification and adaptive
861 behavior prediction of children with autism spectrum disorder based upon multivariate
862 data analysis of markers of oxidative stress and DNA methylation. PLoS Comput Biol.
863 2017;13(3):e1005385. Published 2017 Mar 16. doi:10.1371/journal.pcbi.1005385.
864 36. Hsiao EY, McBride SW, Hsien S, Sharon G, Hyde ER, McCue T, Codelli JA, Chow J,
865 Reisman SE, Petrosino JF, Patterson PH, Mazmanian SK. Microbiota modulate
866 behavioral and physiological abnormalities associated with neurodevelopmental
867 disorders. Cell. 2013 Dec 19;155(7):1451-63. doi: 10.1016/j.cell.2013.11.024. Epub 2013
868 Dec 5. PMID: 24315484; PMCID: PMC3897394.
869 37. Huberty, C. J. (1975). Discriminant analysis. Review of Educational Research, 45(4),
870 543-598.
871 38. Hung, L.Y., Margolis, K.G. Autism spectrum disorders and the gastrointestinal tract:
872 insights into mechanisms and clinical relevance. Nat Rev Gastroenterol Hepatol (2023).
873 https://doi.org/10.1038/s41575-023-00857-1
874 39. Javaneh Tamiji, Dorota A. Crawford. The Neurobiology of Lipid Metabolism in Autism
875 Spectrum Disorders. *Neurosignals* 2011; 18 (2): 98–112.
876 https://doi.org/10.1159/000323189
877 40. Jiang, J., Wang, D., Jiang, Y. et al. The gut metabolite indole-3-propionic acid activates
878 ERK1 to restore social function and hippocampal inhibitory synaptic transmission in a
879 16p11.2 microdeletion mouse model. Microbiome 12, 66 (2024).
880 https://doi.org/10.1186/s40168-024-01755-7
881 41. Joensuu M, Wallis TP, Saber SH, Meunier FA. Phospholipases in neuronal function: A
882 role in learning and memory? J Neurochem. 2020;153(3):300-333. doi:
883 10.1111/jnc.14918. Epub 2020 Feb 7. PMID: 31745996.
884 42. Kang DW, Adams JB, Gregory AC, et al. Microbiota Transfer Therapy alters gut
885 ecosystem and improves gastrointestinal and autism symptoms: an open-label study.
886 *Microbiome*. 2017;5(1):10. doi:10.1186/s40168-016-0225-7.

887 43. Kang D.W., Ilhan Z.E., Isern N.G., Hoyt D.W., Howsmon D.P., Shaffer M., Lozupone
888 C.A., Hahn J., Adams J.B., Krajmalnik-Brown R. Differences in fecal microbial
889 metabolites and microbiota of children with autism spectrum disorders. Anaerobe.
890 2018;49:121–131. doi:10.1016/j.anaerobe.2017.12.007.
891 44. Kang DW, Adams JB, Coleman DM, Pollard EL, Maldonado J, McDonough-Means S,
892 Caporaso JG, Krajmalnik-Brown R. Long-term benefit of Microbiota Transfer Therapy
893 on autism symptoms and gut microbiota. Sci Rep. 2019 Apr 9;9(1):5821. doi:
894 10.1038/s41598-019-42183-0. PMID: 30967657; PMCID: PMC6456593.
895 45. Kang DW, Adams JB, Vargason T, Santiago M, Hahn J, Krajmalnik-Brown R. Distinct
896 Fecal and Plasma Metabolites in Children with Autism Spectrum Disorders and Their
897 Modulation after Microbiota Transfer Therapy. Marco ML, ed. *mSphere*.
898 2020;5(5):e00314-20. doi:10.1128/mSphere.00314-20.
899 46. Khalifa D, Shahin O, Salem D, Raafat O. Serum glutamate was elevated in children aged
900 3-10 years with autism spectrum disorders when they were compared with controls. Acta
901 Paediatr. 2019 Feb;108(2):295-299. doi: 10.1111/apa.14477. Epub 2018 Jul 16. PMID:
902 29949195.
903 47. Krajmalnik-Brown R, Lozupone C, Kang D-W, Adams JB. Gut bacteria in children with
904 autism spectrum disorders: challenges and promise of studying how a complex
905 community influences a complex disease. Microb Ecol Health Dis. 2015; 26.
906 doi:10.3402/mehd.v26.26914.
907 48. Kumar A, Pramanik J, Goyal N, et al. Gut Microbiota in Anxiety and Depression:
908 Unveiling the Relationships and Management Options. *Pharmaceuticals (Basel)*.
909 2023;16(4):565. Published 2023 Apr 9. doi:10.3390/ph16040565
910 49. Leyrolle Q, Prado-Perez L, Layé S. The gut-derived metabolites as mediators of the
911 effect of healthy nutrition on the brain. Front Nutr. 2023 Jun 9;10:1155533. doi:
912 10.3389/fnut.2023.1155533. PMID: 37360297; PMCID: PMC10289296.
913 50. Li C, Shen K, Chu L, Liu P, Song Y, Kang X. Decreased levels of urinary free amino
914 acids in children with autism spectrum disorder. J Clin Neurosci. 2018 Aug;54:45-49.
915 doi: 10.1016/j.jocn.2018.05.001. Epub 2018 May 28. PMID: 29853226.
916 51. Lin S, Yue X, Wu H, Han T-L, Zhu J, Wang C, et al. Explore potential plasma biomarkers
917 of acute respiratory distress syndrome (ARDS) using GC-MS metabolomics

52. Lombard J, Autism: a mitochondrial disorder? Med. Hypotheses 50, 497–500 (1998). – PubMed
53. Lord C, Elsabbagh M, Baird G, Veenstra-Vanderweele J. Autism spectrum disorder. Lancet. 2018 Aug 11;392(10146):508-520. doi: 10.1016/S0140-6736(18)31129-2. Epub 2018 Aug 2. PMID: 30078460; PMCID: PMC7398158.
54. Martin CR, Osadchiy V, Kalani A, Mayer EA. The Brain-Gut-Microbiome Axis. Cell Mol Gastroenterol Hepatol. 2018;6(2):133-148. Published 2018 Apr 12. doi:10.1016/j.jcmgh.2018.04.003
55. Morton JT, Jin DM, Mills RH, et al. Multi-level analysis of the gut–brain axis shows autism spectrum disorder-associated molecular and microbial profiles. Nat Neurosci. 2023;26(7):1208-1217. doi:10.1038/s41593-023-01361-0
56. Mottron, L., Bzdok, D. Autism spectrum heterogeneity: fact or artifact?. Mol Psychiatry 25, 3178–3185 (2020). https://doi.org/10.1038/s41380-020-0748-y.
57. Mussap, M., Siracusano, M., Noto, A., Fattuoni, C., Riccioni, A., Rajula, H. S. R., Fanos, V., Curatolo, P., Barberini, L., & Mazzone, L. (2020). The Urine Metabolome of Young Autistic Children Correlates with Their Clinical Profile Severity. Metabolites, 10(11), 476. https://doi.org/10.3390/metabo10110476.
58. Needham BD, Adame MD, Serena G, Rose DR, Preston GM, Conrad MC, Campbell AS, Donabedian DH, Fasano A, Ashwood P, Mazmanian SK. Plasma and Fecal Metabolite Profiles in Autism Spectrum Disorder. Biol Psychiatry. 2021 Mar 1;89(5):451-462. doi: 10.1016/j.biopsych.2020.09.025. Epub 2020 Oct 10. PMID: 33342544; PMCID: PMC7867605.
59. Osredkar, J., Baškovič, B. Ž., Finderle, P., Bobrowska-Korczak, B., Gątarek, P., Rosiak, A., Giebułtowicz, J., Vrhovšek, M. J., & Kałużna-Czaplińska, J. (2023). Relationship between Excreted Uremic Toxins and Degree of Disorder of Children with ASD. International Journal of Molecular Sciences, 24(8), 7078. https://doi.org/10.3390/ijms24087078
60. Pastural E, Ritchie S, Lu Y, Jin W, Kavianpour A, Khine Su-Myat K, Heath D, Wood PL, Fisk M, Goodenowe DB. Novel plasma phospholipid biomarkers of autism: mitochondrial dysfunction as a putative causative mechanism. Prostaglandins Leukot

Essent Fatty Acids. 2009 Oct;81(4):253-64. doi: 10.1016/j.plefa.2009.06.003. Epub 2009 Jul 15. PMID: 19608392.

61. Peralta-Marzal LN, Prince N, Bajic D, Roussin L, Naudon L, Rabot S, Garssen J, Kraneveld AD, Perez-Pardo P. The Impact of Gut Microbiota-Derived Metabolites in Autism Spectrum Disorders. Int J Mol Sci. 2021 Sep 17;22(18):10052. doi: 10.3390/ijms221810052. PMID: 34576216; PMCID: PMC8470471.
62. Peralta-Marzal, L.N., Rojas-Velazquez, D., Rigters, D. et al. A robust microbiome signature for autism spectrum disorder across different studies using machine learning. Sci Rep 14, 814 (2024). https://doi.org/10.1038/s41598-023-50601-7.
63. Persico, A. M., & Napolioni, V. (2013). Urinary p-cresol in autism spectrum disorder. Neurotoxicology and Teratology, 36, 82–90. https://doi.org/10.1016/j.ntt.2012.09.002.
64. Petroff O.A.C. Book Review: GABA and glutamate in the human brain. Neuroscientist. 2002;8:562–573.
65. Petroff OA. GABA and glutamate in the human brain. Neuroscientist. 2002 Dec;8(6):562-73. doi: 10.1177/1073858402238515. PMID: 12467378.
66. Piras, C., Mussap, M., Noto, A., De Giacomo, A., Cristofori, F., Spada, M., Fanos, V., Atzori, L., & Francavilla, R. (2022). Alterations of the Intestinal Permeability are Reflected by Changes in the Urine Metabolome of Young Autistic Children: Preliminary Results. Metabolites, 12(2), 104. https://doi.org/10.3390/metabo12020104.
67. Qureshi, F.; Adams, J.; Hanagan, K.; Kang, D.-W.; Krajmalnik-Brown, R.; Hahn, J. Multivariate Analysis of Fecal Metabolites from Children with Autism Spectrum Disorder and Gastrointestinal Symptoms before and after Microbiota Transfer Therapy. *J. Pers. Med.* **2020**, *10*, 152. https://doi.org/10.3390/jpm10040152
68. Rossignol DA, Frye RE, Mitochondrial dysfunction in autism spectrum disorders: a systematic review and meta-analysis. Mol. Psychiatry 17, 290–314 (2012). - PMC – PubMed
69. Sagaro GG, Traini E, Amenta F. Activity of Choline Alphoscerate on Adult-Onset Cognitive Dysfunctions: A Systematic Review and Meta-Analysis. J Alzheimers Dis. 2023;92(1):59-70. doi: 10.3233/JAD-221189. PMID: 36683513; PMCID: PMC10041421.

70. Saito Y, Sato T, Nomoto K, Tsuji H. Identification of phenol- and p-cresol-producing intestinal bacteria by using media supplemented with tyrosine and its metabolites. FEMS Microbiol Ecol. 2018 Sep 1;94(9):fiy125. doi: 10.1093/femsec/fiy125. Erratum in: FEMS Microbiol Ecol. 2019 Apr 1;95(4): Erratum in: FEMS Microbiol Ecol. 2020 Jan 1;96(1): PMID: 29982420; PMCID: PMC6424909.
71. Selma MV, Beltrán D, García-Villalba R, Espín JC, Tomás-Barberán FA. Description of urolithin production capacity from ellagic acid of two human intestinal Gordonibacter species. Food Funct. 2014;5(8):1779-1784. doi:10.1039/c4fo00092g
72. Serger, E., Luengo-Gutierrez, L., Chadwick, J.S. et al. The gut metabolite indole-3 propionate promotes nerve regeneration and repair. Nature 607, 585–592 (2022). https://doi.org/10.1038/s41586-022-04884-x
73. Shinohe A, Hashimoto K, Nakamura K, et al. Increased serum levels of glutamate in adult patients with autism. *Prog Neuropsychopharmacol Biol Psychiatry*. 2006;30(8):1472-1477. doi:10.1016/j.pnpbp.2006.06.013
74. Spanogiannopoulos P, Bess EN, Carmody RN, Turnbaugh PJ. The microbial pharmacists within us: a metagenomic view of xenobiotic metabolism. Nat Rev Microbiol. 2016 Apr;14(5):273-87. doi: 10.1038/nrmicro.2016.17. Epub 2016 Mar 14. PMID: 26972811; PMCID: PMC5243131.
75. Stewart Campbell A, Needham BD, Meyer CR, Tan J, Conrad M, Preston GM, Bolognani F, Rao SG, Heussler H, Griffith R, Guastella AJ, Janes AC, Frederick B, Donabedian DH, Mazmanian SK. Safety and target engagement of an oral small-molecule sequestrant in adolescents with autism spectrum disorder: an open-label phase 1b/2a trial. Nat Med. 2022 Mar;28(3):528-534. doi: 10.1038/s41591-022-01683-9. Epub 2022 Feb 14. PMID: 35165451.
76. Szeligowski T, Yun AL, Lennox BR, Burnet PWJ. The Gut Microbiome and Schizophrenia: The Current State of the Field and Clinical Applications. *Front Psychiatry*. 2020;11:156. Published 2020 Mar 12. doi:10.3389/fpsyt.2020.00156
77. Tamiji J, Crawford DA. The neurobiology of lipid metabolism in autism spectrum disorders. Neurosignals. 2010;18(2):98-112. doi:10.1159/000323189
78. Tamji, R., & Crawford, M. A. (2011). Phospholipid metabolism and mitochondrial function. *International Journal of Developmental Neuroscience*, 29(6), 633-641.

1009 79. Takyi, E., Nirmalkar, K., Adams, J., & Krajmalnik-Brown, R. (2025). Interventions
1010 targeting the gut microbiota and their possible effect on gastrointestinal and
1011 neurobehavioral symptoms in autism spectrum disorder. Gut Microbes, 17(1).
1012 https://doi.org/10.1080/19490976.2025.2499580
1013 80. Tevzadze, G., Shanshiashvilli, L., & Mikeladze, D. (2017). Children with epilepsy and
1014 autistic spectrum disorders show similarly high levels of urinary p-cresol. Journal of
1015 Biological Physics and Chemistry, 17(2), 77–80.
1016 https://doi.org/10.4024/05te17a.jbpc.17.02.
1017 81. Timperio, A. M., Gevi, F., Cucinotta, F., Ricciardello, A., Turriziani, L., Scattoni, M. L.,
1018 & Persico, A. M. (2022). Urinary Untargeted Metabolic Profile Differentiates Children
1019 with Autism from Their Unaffected Siblings. Metabolites, 12(9).
1020 https://doi.org/10.3390/metabo12090797.
1021 82. Traini E, Carotenuto A, Fasanaro AM, Amenta F. Volume Analysis of Brain Cognitive
1022 Areas in Alzheimer's Disease: Interim 3-Year Results from the ASCOMALVA Trial. J
1023 Alzheimers Dis. 2020;76(1):317-329. doi: 10.3233/JAD-190623. PMID: 32508323;
1024 PMCID: PMC7369051.
1025 83. Tsai GC, Lane HY, Yang PC, Chong MY, Lange N. 2004. Glycine transporter I inhibitor,
1026 N-methylglycine (Sarcosine), added to antipsychotics for the treatment of schizophrenia.
1027 Biol Psychiatry 55:452–456.
1028 84. Vargason T, Roth E, Grivas G, Ferina J, Frye RE, Hahn J. Classification of autism
1029 spectrum disorder from blood metabolites: Robustness to the presence of co-occurring
1030 conditions. Res Autism Spectr Disord. 2020;77:101644. doi:10.1016/j.rasd.2020.101644.
1031 85. Venkatesh M, Mukherjee S, Wang H, Li H, Sun K, Benechet AP, Qiu Z, Maher L,
1032 Redinbo MR, Phillips RS, Fleet JC, Kortagere S, Mukherjee P, Fasano A, Le Ven J,
1033 Nicholson JK, Dumas ME, Khanna KM, Mani S. Symbiotic bacterial metabolites
1034 regulate gastrointestinal barrier function via the xenobiotic sensor PXR and Toll-like
1035 receptor 4. Immunity. 2014 Aug 21;41(2):296-310. doi: 10.1016/j.immuni.2014.06.014.
1036 Epub 2014 Jul 24. PMID: 25065623; PMCID: PMC4142105.
1037 86. Ventura G, Calvano CD, Porcelli V, et al. Phospholipidomics of peripheral blood
1038 mononuclear cells (PBMCs): the tricky case of children with autism spectrum disorder

1039 (ASD) and their healthy siblings. Anal Bioanal Chem. 2020;412(25):6859-6874.
1040 doi:10.1007/s00216-020-02817-z
1041 87. Wang, H.; Liang, S.; Wang, M.; Gao, J.; Sun, C.; Wang, J.; Xia, W.; Wu, S.; Sumner, S.J.;
1042 Zhang, F.; et al. Potential Serum Biomarkers from a Metabolomics Study of Autism. *J.*
1043 *Psychiatry Neurosci.* **2016**, *41*, 27–37.
1044 88. Wang, T., Chen, B., Luo, M. et al. Microbiota-indole 3-propionic acid-brain axis mediates
1045 abnormal synaptic pruning of hippocampal microglia and susceptibility to ASD in IUGR
1046 offspring. Microbiome 11, 245 (2023). https://doi.org/10.1186/s40168-023-01656-1
1047 89. Wouter G. Touw, Jumamurat R. Bayjanov, Lex Overmars, Lennart Backus, Jos
1048 Boekhorst, Michiel Wels, Sacha A. F. T. van Hijum, Data mining in the Life Sciences
1049 with Random Forest: a walk in the park or lost in the jungle?, Briefings in
1050 Bioinformatics, Volume 14, Issue 3, May 2013, Pages 315–326,
1051 https://doi.org/10.1093/bib/bbs034
1052 90. Yu R, Wu Z, Wang S, Zhang M, Zhou G, Li B. Isolation, identification and
1053 characterization of propionic acid bacteria associated with autistic spectrum disorder.
1054 Microb Pathog. 2020 Oct;147:104371. doi: 10.1016/j.micpath.2020.104371. Epub 2020
1055 Jul 4. PMID: 32634613. \
1056 91. Zhao, ZH., Xin, FZ., Xue, Y. et al. Indole-3-propionic acid inhibits gut dysbiosis and
1057 endotoxin leakage to attenuate steatohepatitis in rats. Exp Mol Med 51, 1–14 (2019).
1058 https://doi.org/10.1038/s12276-019-0304-5
1059 92. Zheng Y, Bek MK, Prince NZ, Peralta Marzal LN, Garssen J, Perez Pardo P, Kraneveld
1060 AD. The Role of Bacterial-Derived Aromatic Amino Acids Metabolites Relevant in
1061 Autism Spectrum Disorders: A Comprehensive Review. Front Neurosci. 2021 Oct
1062 21;15:738220. doi: 10.3389/fnins.2021.738220. PMID: 34744609; PMCID:
1063 PMC8568365.
1064 93. Zheng Y, Prince N, van Hattem C, Garssen J, Pardo PP, Kraneveld AD. The interaction
1065 between intestinal bacterial metabolites and phosphatase and tensin homolog in autism
1066 spectrum disorder. Mol Cell Neurosci. 2023 Mar;124:103805. doi:
1067 10.1016/j.mcn.2022.103805. Epub 2022 Dec 30. PMID: 36592799.
1068 94. Zhou Y, Bi Z, Hamilton MJ, Zhang L, Su R, Sadowsky MJ, Roy S, Khoruts A, Chen
1069 C. *p*-Cresol Sulfate Is a Sensitive Urinary Marker of Fecal Microbiota Transplantation

1070 and Antibiotics Treatments in Human Patients and Mouse Models. *International Journal*
1071 *of Molecular Sciences*. 2023; 24(19):14621. https://doi.org/10.3390/ijms241914621